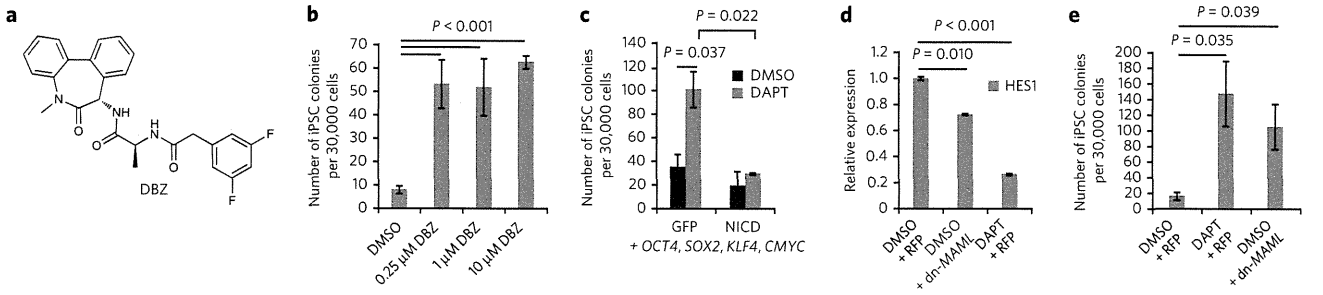

Figure 2 | γ-secretase inhibition promotes reprogramming by blocking Notch signaling. (**a**) Chemical structure of DBZ. (**b**) The efficiency of NANOG+/TRA-1-81+ iPSC generation from human neonatal keratinocytes transduced with *OCT4*, *KLF4*, *SOX2* and *CMYC* and treated with different concentrations of DBZ from days 1-18 after transduction. (**c**) The efficiency of NANOG+/ TRA-1-81+ iPSC generation from human neonatal keratinocytes transduced with *OCT*, *SOX2*, *KLF4* and *CMYC* and GFP or NOTCH intracellular domain (NICD) and treated with DMSO or 10 μM DAPT from days 1-18 after transduction. Cells were transduced with NOTCH ICD or GFP lentivirus 1 day after transduction with the reprogramming factors. (**d**) qPCR analysis of expression levels of NOTCH-dependent gene HES1 in human neonatal keratinocytes transduced with dominant-negative MASTERMIND-LIKE-1 (dn-*MAML1*) or RFP. (**e**) The efficiency of NANOG+/TRA-1-81+ iPSC generation from human neonatal keratinocytes transduced with *OCT*, *SOX2*, *KLF4* and *CMYC* and RFP or dn-*MAML1* and treated with DMSO or 10 μM DAPT from days 1-18 after transduction. For all experiments, error bars represent the s.d. between two or three biological replicates, and statistical significance was determined using a two-tailed homoscedastic Student's *t*-test.

reductions in the levels of the intracellular domain of the NOTCH receptor (**Supplementary Fig. 1a**) and the NOTCH-dependent genes *HES1* and *HES5* (**Supplementary Fig. 3a**), indicating that DBZ administration inhibited NOTCH signaling. Consistent with the notion that NOTCH inhibition increases the rate of reprogramming, DBZ stimulated the formation of human iPSC colonies (**Fig. 2b**).

Both DBZ and DAPT could have effects on the processing of unidentified γ-secretase substrates that are distinct from NOTCH, which might also affect reprogramming efficiency. If the beneficial effects of DAPT on reprogramming were being mediated through the specific inhibition of NOTCH signaling rather than through some other target of γ-secretase, then we reasoned that constitutive activation of NOTCH signaling should eliminate the beneficial effect

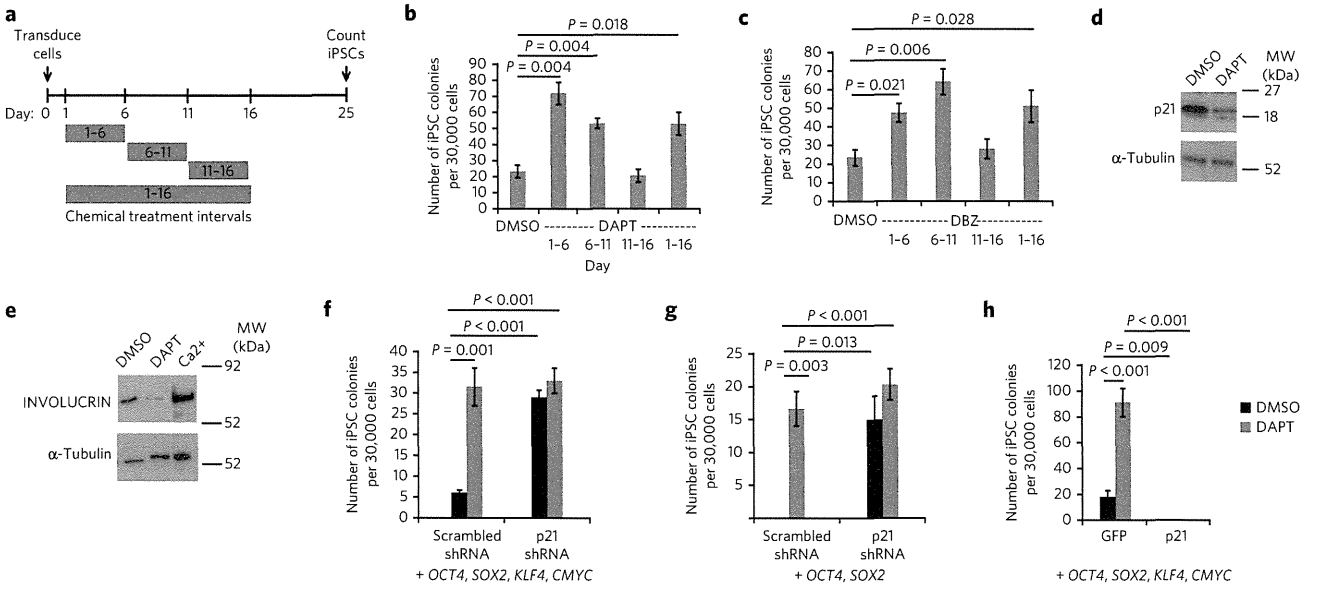

Figure 3 | Notch inhibition promotes keratinocyte reprogramming by suppressing p21. (**a**) Schematic of the DAPT treatment time course on human neonatal keratinocytes. (**b**,**c**) Efficiency of NANOG+/TRA-1-81+ iPSC generation from human neonatal keratinocytes transduced with *OCT4*, *SOX2*, *KLF4* and *CMYC* and treated with intervals of 10 μM DAPT (**b**) or 2 μM DBZ (**c**). (**d**) Western blot for p21 in human neonatal keratinocytes transduced with *OCT4* and *SOX2* and treated with DMSO or 10 μM DAPT. The full blot is shown in **Supplementary Figure 7c**. (**e**) Western blot for INVOLUCRIN in human neonatal keratinocytes treated with DMSO, 10 μM DAPT or 1.2 mM calcium chloride for 6 d. Calcium was used as a positive control to induce keratinocyte differentiation. The full blot is shown in **Supplementary Figure 7d**. (**f**) Efficiency of NANOG+/TRA-1-81+ iPSC generation from human neonatal keratinocytes transduced with *OCT4*, *KLF4*, *SOX2* and *CMYC* and a scrambled shRNA or a p21 shRNA at day 0 of reprogramming. DAPT was added at 10 μM. (**g**) Efficiency of NANOG+/TRA-1-81+ iPSC generation from human neonatal keratinocytes transduced with *OCT4* and *SOX2* and a scrambled shRNA control or a p21 shRNA at day 0 of reprogramming. DAPT was added at 2.5 μM. (**h**) Efficiency of NANOG+/TRA-1-81+ iPSC generation from human neonatal keratinocytes transduced with *OCT*, *SOX2*, *KLF4* and *CMYC* and GFP or p21 and treated with DMSO or 10 μM DAPT from days 1-18 after transduction. For all experiments, error bars represent the s.d. between two or three biological replicates, and statistical significance was determined using a two-tailed homoscedastic Student's *t*-test.

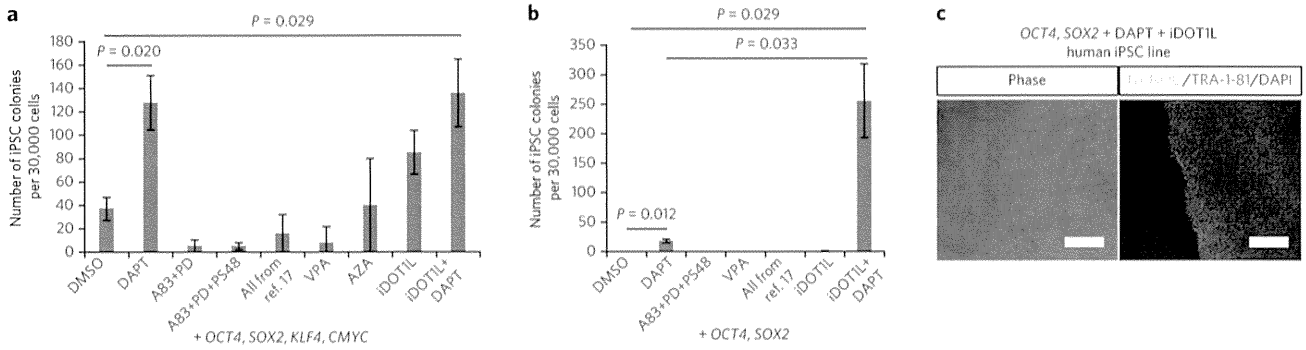

Figure 4 | Highly efficient reprogramming with NOTCH and DOT1L inhibition. (**a**) Comparison of NANOG+/TRA-1-81+ iPSC generation from *OCT4*, *SOX2*, *KLF4* and *CMYC*-transduced human neonatal keratinocytes using 10 μM DAPT versus other published reprogramming chemicals. A83, A8301 (0.5 μM); PD, PD0325901 (0.5 μM); 'All from ref. 17', A8301 (0.5 μM), PD0325901 (0.5 μM), PS48 (5 μM), sodium butyrate (0.25 mM), Parnate (2 μM) and CHIR99021 (3 μM); AZA, 5-aza-cytidine (0.5 μM); VPA, valproic acid (0.5 mM); iDOT1L, EPZ004777 (3 μM). (**b**) Comparison of NANOG+/TRA-1-81+ iPSC generation from *OCT4*- and *SOX2*- transduced human neonatal keratinocytes using 2.5 μM DAPT versus other published reprogramming chemicals. (**c**) iPSC line generated from human neonatal keratinocytes using *OCT4*, *SOX2*, DAPT and iDOT1L. Scale bars, 100 μm. For all experiments, error bars represent the s.d. between two or three biological replicates, and statistical significance was determined using a two-tailed homoscedastic Student's *t*-test.

of DAPT. Consistent with this notion, we found that overexpression of the NOTCH intracellular domain (**Supplementary Fig. 3b**) stimulated the expression of NOTCH-target genes (**Supplementary Fig. 3c**) and completely blocked the positive effects of DAPT on reprogramming (**Fig. 2c**). Conversely, we reasoned that antagonizing the transcriptional activity of NOTCH should increase the rate of keratinocyte reprogramming. Indeed, when we suppressed NOTCH activity by overexpressing a dominant-negative form of *MAML1* (**Fig. 2d**), a transcriptional co-activator for NOTCH[36,37], we observed an increase in iPSC generation from keratinocytes transduced with all four reprogramming factors (**Fig. 2e**). Therefore, we conclude that the inhibition of NOTCH signaling promotes the reprogramming of both human and mouse keratinocytes.

To understand how Notch inhibition promotes iPSC generation, we first determined when in the reprogramming process it was required. We treated mouse keratinocytes with DAPT either before or both before and after transduction with reprogramming factors. Although treatment both before and after transduction yielded a fourfold increase in iPSC generation, we found that pretreatment alone resulted in a 2.5-fold enhancement in reprogramming efficiency (**Supplementary Fig. 4a**). To more precisely pinpoint the effective post-transduction treatment window, we transduced human keratinocytes with *KLF4*, *OCT4*, *SOX2* and *CMYC* and administered DAPT or DBZ from days 1–6, 6–11, 11–16 or 1–16 after viral infection (**Fig. 3a–c**). Chemical inhibition of NOTCH signaling was most effective during early time points, increasing iPSC generation when used from days 1–6 and 6–11 (**Fig. 3b,c**). In contrast, a later treatment from days 11–16 had little effect on reprogramming (**Fig. 3b,c**). Together, these results indicate that Notch inhibition can act on the starting keratinocytes and at early time points just after the initiation of transcription factor overexpression to enhance reprogramming.

Notch inhibition acts by suppressing p21 expression

One way that Notch inhibition could promote iPSC formation is by activating the expression of the reprogramming transcription factors from their endogenous loci. However, when we treated human keratinocytes with DAPT and analyzed their gene expression, we found that levels of *KLF4*, *OCT4* and *CMYC* actually decreased, and *SOX2* levels did not change (**Supplementary Fig. 4b**).

In the mammalian epidermis, Notch signaling functions as a switch that directly activates *p21* transcription, which in turn forces keratinocytes to exit the cell cycle and begin differentiating[38]. To determine whether chemical inhibition of Notch signaling in keratinocytes might be enhancing their reprogramming potential by suppressing *p21*, we measured p21 levels in human keratinocytes in the presence and absence of DAPT. Consistent with previous reports[38], we found that Notch inhibition decreased the levels of *p21* mRNA and protein in these cells (**Fig. 3d** and **Supplementary Fig. 4c**). In addition, DAPT treatment slightly decreased the level of Flag-tagged p21 protein expressed by an exogenous retrovirus, indicating that Notch may also regulate p21 after transcription (**Supplementary Fig. 4d,e**). Consistent with these observations, Notch inhibition suppressed expression of INVOLUCRIN, which is expressed in more differentiated keratinocytes (**Fig. 3e**).

To verify that Notch inhibition promotes iPSC reprogramming by suppressing p21, we performed two-factor (*Oct4* and *Sox2*) and four-factor reprogramming in keratinocytes with p21 siRNA and shRNA in the presence or absence of DAPT. Mouse keratinocytes transduced with *Klf4*, *Sox2*, *Oct4* and *cMyc* showed a similar increase in iPSC generation when treated with either 2.5 μm DAPT or p21 siRNA (**Supplementary Fig. 4f**). The efficiency of reprogramming with these two methods was not measurably different (**Supplementary Fig. 4f**), and treating with DAPT in the presence of the p21 siRNA did not produce a demonstrable increase in iPSC formation (**Supplementary Fig. 4f**). Similarly, suppression of p21 by shRNA (**Supplementary Fig. 4g,h**) enabled the generation of iPSCs from human keratinocytes transduced with two or four factors at rates equivalent to DAPT treatment (**Fig. 3f,g**). Again, supplementing p21 knockdown with DAPT treatment did not result in an increase in iPSC formation (**Fig. 3f,g**). These results indicate that p21 suppression and DAPT have similar effects on iPSC generation from keratinocytes and that DAPT does not provide an additional advantage over p21 suppression alone.

If Notch inhibition and p21 suppression indeed blocks keratinocyte differentiation, the p21-treated keratinocytes would be predicted to display an increase in their long-term proliferative capacity[39]. The ability to form large colonies on collagen demonstrates the ability of keratinocytes to self-renew extensively and is a functional property unique to undifferentiated cells of this lineage[39]. In contrast, differentiated keratinocytes senesce after only a few rounds of division and do not form colonies[39]. DAPT treatment of human keratinocytes for 6 d markedly increased the number of cells capable of forming large colonies when cultured for an additional 14 d in the absence of the chemical (**Supplementary Fig. 4i**). The resulting fourfold increase in colony formation rate

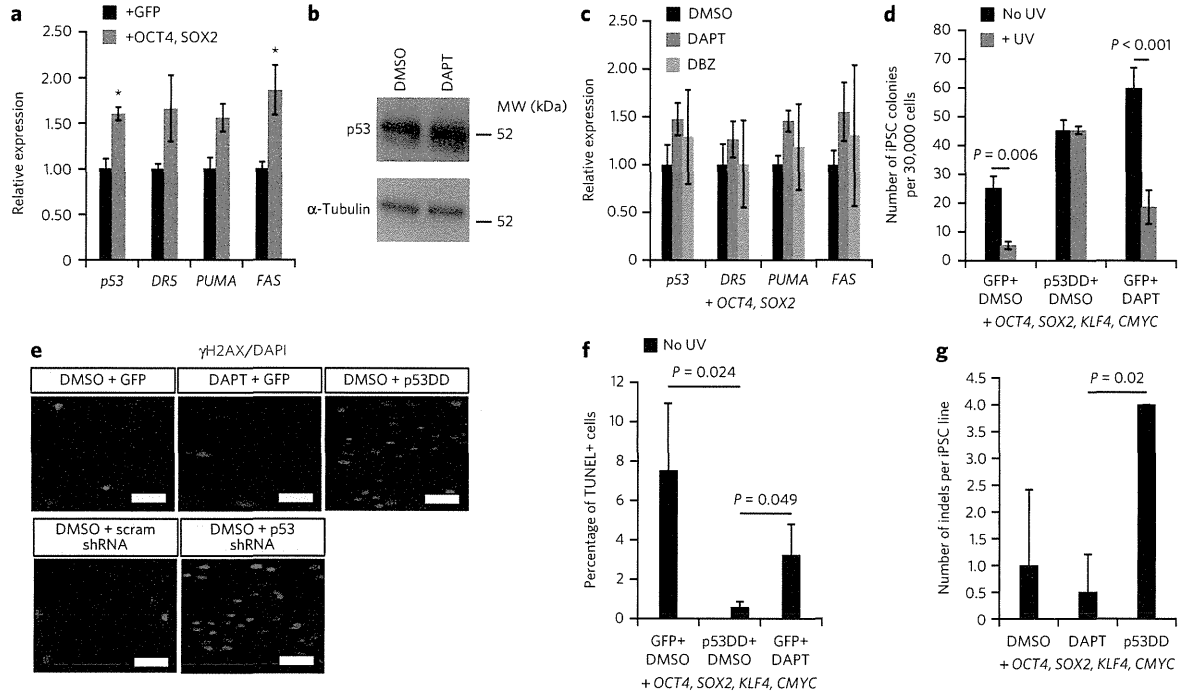

Figure 5 | NOTCH inhibition suppresses p21 without reducing p53 activity. (**a**) qPCR analysis of p53-dependent genes in human neonatal keratinocytes 3 d after transduction of GFP or *OCT4* and *SOX2*. (**b**) Western blot of p53 levels in human neonatal keratinocytes with DMSO or 10 μM DAPT treatment for 3 d. The full blot is shown in **Supplementary Figure 7g**. (**c**) qPCR analysis of p53-dependent genes after 10 μM DAPT or 2 μM DBZ treatment for 3 d in *OCT4*, *SOX2*-transduced human keratinocytes. (**d**) The efficiency of NANOG+/TRA-1-81+ iPSC generation in *OCT4*, *SOX2*, *KLF4* and *CMYC*-transduced human neonatal keratinocytes transduced with p53DD or GFP with or without exposure to UV irradiation. (**e**) γH2AX immunostaining in human neonatal keratinocytes 10 d after transduction with *OCT4*, *SOX2*, *KLF4* and *CMYC* and treatment with DAPT, p53DD or p53 shRNA. Scale bars, 50 μm. (**f**) The percentage of TUNEL-positive cells in human neonatal keratinocyte reprogramming cultures with active or inactive p53 (p53DD expression) 10 d after transduction with *OCT4*, *SOX2*, *KLF4* and *CMYC*. (**g**) The number of insertions or deletions (indels) per iPSC line derived under normal, DAPT or p53DD conditions, as determined by array comparative genomic hybridization (CGH). For all experiments, error bars represent the s.d. between two biological replicates, and statistical significance was determined using a two-tailed homoscedastic Student's *t*-test. $^*P < 0.05$.

was similar in magnitude to the elevation in iPSC generation with DAPT treatment (**Fig. 1b**). To determine whether this increased self-renewal capacity was indeed promoting reprogramming, we transduced keratinocytes with p21 to limit their replication and attempted to reprogram them either with or without DAPT. The forced p21 expression severely impaired the self-renewal potential of the keratinocytes (**Supplementary Fig. 4j**) and inhibited iPSC formation after transduction with the four reprogramming factors and treatment with DAPT (**Fig. 3h**).

Because Notch inhibition does not promote fibroblast replication[40], if this is the mechanism by which DAPT improves reprogramming, we would not expect chemical treatment to affect mouse embryonic fibroblast[41] reprogramming[41]. Indeed, DAPT treatment of MEFs transduced with all four reprogramming factors did not affect the rate of iPSC generation (**Supplementary Fig. 4k**). Together, these results demonstrate that Notch inhibition promotes iPSC generation from keratinocytes by repressing their differentiation and enhancing their long-term replicative potential through p21 suppression.

Efficient reprogramming with Notch and DOT1L inhibition

Knowing that Notch inhibition enhances iPSC generation through this unique mechanism, we next wanted to compare its activity to previously described reprogramming molecules that act through other mechanisms[17,42–44] and identify any that DAPT might synergize with. When we transduced human neonatal keratinocytes with *KLF4*, *SOX2*, *OCT4* and *CMYC* and treated them with various combinations of compounds shown to enhance reprogramming in other reports, including an activator of 3′-phosphoinositide-dependent kinase-1 (ref. 17); inhibitors of TGF-β, MEK and GSK3β signaling[17]; histone deacetylase inhibitors[17,42]; histone methyltransferase inhibitors[17,44]; and a DNA methyltransferase inhibitor[43], we found that DAPT treatment was the most potent at enhancing reprogramming (**Fig. 4a**). This remained true when we attempted reprogramming with only *OCT4* and *SOX2* (**Fig. 4b**).

However, an inhibitor of the histone methyltransferase DOT1L (iDOT1L) synergized *OCT4*, *SOX2* and DAPT to elevate the rate of iPSC generation by tenfold over the rate with *OCT4*, *SOX2* and DAPT alone, making it even more efficient than four-factor reprogramming either with or without DAPT (**Fig. 4b**). The *OCT4*+ *SOX2*+ DAPT+ iDOT1L colonies could be readily expanded and maintained NANOG and TRA-1-81 expression (**Fig. 4c**). These data indicate that Notch inhibition is a potent enhancer of reprogramming in keratinocytes that can synergize with chromatin-modifying compounds to induce pluripotency at a high efficiency with only *OCT4* and *SOX2*.

Notch inhibition does not compromise p53 activity

Previous studies of p53 and p21 in reprogramming have suggested that ectopic overexpression of reprogramming transcription factors can activate p53, which then induces either apoptosis or the expression of p21, thus inhibiting reprogramming[3,6]. Because suppression of the p53 pathway greatly facilitates iPSC generation, this approach has become an important part of reprogramming methods that reduce or eliminate integrating exogenous transcription factors[3,4]. However, because p53 inhibition allows the accumulation of

genetic mutations during reprogramming[8], alternative approaches for increasing reprogramming efficiencies would be desirable. We therefore next asked whether Notch inhibition promotes reprogramming through a p53-dependent or p53-independent pathway by analyzing the effects of DAPT and DBZ treatment on p53 and its target genes. First, we confirmed the finding that transduction with the iPSC reprogramming factors stimulated p53 activity (**Fig. 5a**). Chemical inhibition of Notch signaling in both human and mouse keratinocytes did not reduce the expression of p53 at the protein or mRNA level either before or after transduction with the reprogramming factors (**Fig. 5b,c** and **Supplementary Fig. 5a,b**). Moreover, transcriptional analysis of DAPT-treated human and mouse keratinocytes revealed that the mRNA levels of the p53 target genes *Tnfrsf10b* (also known as *Dr5*), *Bbc3* (also known as *Puma*) and *Fas* were not decreased (**Fig. 5c** and **Supplementary Fig. 5a,b**), supporting the notion that p53 activity was not suppressed by Notch inhibition.

To further confirm that DAPT treatment did not suppress p53 activity, we performed reprogramming experiments with and without DAPT after UV irradiation. UV exposure causes DNA damage, which in turn reduces reprogramming efficiencies by inducing p53-dependent apoptosis[8]. However, p53-deficient cells are resistant to the negative effects of UV irradiation on reprogramming[8]. Therefore, if p53 activity was maintained in DAPT-treated cultures, then we would expect a sharp decrease in reprogramming efficiency after UV irradiation. As a control for p53 deficiency, we performed four-factor reprogramming with or without UV irradiation using keratinocytes in which we overexpressed a dominant-negative form of p53 (p53DD)[3] that suppressed p53 activity, as evidenced by a decrease in the expression levels of p53-dependent target genes (**Supplementary Fig. 5c**). As expected, UV exposure did not affect the rate of iPSC generation when p53DD was expressed, functionally demonstrating that p53 activity was indeed impaired (**Fig. 5d**). In contrast, in the absence of p53DD overexpression, UV exposure sharply reduced the number of iPSCs generated in DMSO-treated cultures (**Fig. 5d**). Similarly, UV irradiation severely diminished the number of iPSC colonies in DAPT-treated cultures, again suggesting that Notch inhibition does not suppress p53 activity during reprogramming (**Fig. 5d**).

Although the difference in reprogramming efficiency in p53-deficient versus DAPT-treated keratinocytes was clearly evident when UV irradiation was used to induce DNA damage, we next determined whether DNA damage was measurably influenced by DAPT treatment under normal reprogramming conditions. To test this, we quantified phosphorylated histone H2AX (γH2AX) expression in four-factor-transduced human keratinocytes treated with DAPT, p53DD or p53 shRNA. Histone H2AX becomes phosphorylated in response to double-stranded DNA breaks, making it a reliable marker of DNA damage[8]. Pan-nuclear γH2AX expression results from replication-induced damage and could indicate insults sustained during reprogramming[8]. We found that 10 d after transduction, pan-nuclear γH2AX staining was greatly elevated in cultures treated with p53DD or p53 shRNA, which is consistent with a previous study in which elevated rates of DNA damage were observed in p53-deficient cells during reprogramming and in the resulting iPSCs[8] (**Fig. 5e** and **Supplementary Fig. 5d–f**). The DAPT-treated cells, however, maintained low cell numbers with pan-nuclear γH2AX expression that were similar to numbers in the control cultures (**Fig. 5e** and **Supplementary Fig. 5f**). These results suggest that, in contrast to p53 deficiency, DAPT treatment did not promote the survival and reprogramming of cells with DNA damage.

To confirm that Notch inhibition does not prevent the apoptosis of compromised cells during reprogramming, we measured the fraction of TUNEL-positive nuclei in DAPT-treated cultures. Despite high rates of DNA damage in the p53-deficient reprogramming cultures, the percentage of TUNEL-positive nuclei was greatly reduced compared to the percentage in a wild-type control, indicating that inactivation of p53 permitted the survival of cells with compromised genomes (**Fig. 5f**). In contrast, the percentage of TUNEL-positive cells was not reduced after DAPT treatment (**Fig. 5f**).

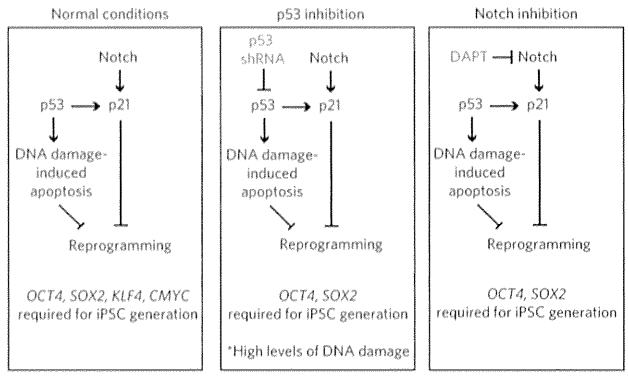

Figure 6 | Model of iPSC generation from human keratinocytes. Notch inhibition allows the production of safer oncogene-free iPSCs by suppressing p21 in a p53-independent manner.

To determine whether DAPT enabled the efficient generation of iPSCs that displayed improved genomic integrity relative to their counterparts made through p53 suppression, we measured the copy number variation in iPSC lines made with DAPT or p53DD. Consistent with the γH2AX and TUNEL staining results, we found that iPSC lines derived in the presence of p53DD had an average of four indels per line, whereas iPSCs derived with a control GFP vector or 10 μm DAPT contained only 1 or 0.5 indels per line, respectively (**Fig. 5g** and **Supplementary Fig. 6**). Together, these experiments show that DNA damage is present during normal reprogramming conditions and that inhibition of p53 allows cells with damaged genomic material to persist. In contrast, Notch inhibition enhances reprogramming without compromising genomic integrity or promoting the survival of iPSCs that have undergone DNA damage.

DISCUSSION

In summary, our findings suggest that signaling through the Notch pathway is a major impediment to the early stages of the reprogramming of both mouse and human keratinocytes into iPSCs (**Fig. 6**). Notably, the mechanism by which Notch signaling most likely inhibits reprogramming of mouse and human cells is by activating p21 independently of p53. Consistent with this hypothesis, treatment of reprogramming cultures with the γ-secretase inhibitors DAPT and DBZ reduced the levels of intracellular Notch and increased colony-forming potential, leading to an increase in the rate of iPSC formation. Suppression of p21 expression by siRNA and shRNA was sufficient to replace Notch inhibition in reprogramming, and exogenous p21 blocked the beneficial effects of DAPT. Notably, the resulting improvement in reprogramming activity did not come at the expense of a reduction in p53 activity or increased genomic instability (**Fig. 6**).

Our findings have immediate and practical ramifications for the improved production of patient-specific human iPSCs. When taken together, our studies show that through pharmacological inhibition of NOTCH, it is routinely possible to produce human iPSCs with only *OCT4* and *SOX2*, rendering *CMYC* and *KLF4* dispensable and thereby reducing the oncogenic potential of the resulting cells. Furthermore, our findings enabled *CMYC*- and *KLF4*-free iPSC production without inhibition of p53 or its target genes involved in apoptosis, allowing proapoptotic pathways that ensure genomic integrity to be engaged[8,10,11]. Thus, in this approach, the production

of oncogene-free iPSC lines does not come at the expense of an increase in mutational load[8,10,11,45].

Studies using nuclear transplantation and defined transcription factors have shown that nuclei become less amenable to reprogramming as they advance developmentally[24–26]. Our study demonstrates that intercellular communication in somatic cultures can cause them to differentiate and lose their reprogramming potential but with small-molecule treatment, it is possible to force them to remain in an undifferentiated, highly reprogrammable state. This approach synergized potently with chemical inactivation of the histone H3 methyltransferase DOT1L, allowing two-factor reprogramming at higher efficiency than with four transcription factors. This indicates that although histone methyltransferase inhibition had almost no effect on the reprogramming of differentiated keratinocytes, it had a profound ability to enhance the reprogramming of undifferentiated keratinocytes. Thus, somatic cells at different developmental stages respond differentially to chromatin-modifying signals during reprogramming. The combined chemical inhibition of NOTCH and DOT1L provides a new approach for boosting the reprogramming potential of keratinocytes and is an attractive starting point for the identification of a small-molecule reprogramming cocktail for human cells.

Accession numbers. Gene Expression Omnibus. Microarray data have been submitted to the GEO repository with accession number GSE35090.

Received 24 September 2013; accepted 13 May 2014; published online 22 June 2014; corrected after print 29 July 2014 and 14 August 2014

METHODS

Methods and any associated references are available in the online version of the paper.

References

1. Aoi, T. *et al.* Generation of pluripotent stem cells from adult mouse liver and stomach cells. *Science* **321**, 699–702 (2008).
2. Nakagawa, M. *et al.* Generation of induced pluripotent stem cells without Myc from mouse and human fibroblasts. *Nat. Biotechnol.* **26**, 101–106 (2008).
3. Kawamura, T. *et al.* Linking the p53 tumour suppressor pathway to somatic cell reprogramming. *Nature* **460**, 1140–1144 (2009).
4. Okita, K. *et al.* A more efficient method to generate integration-free human iPS cells. *Nat. Methods* **8**, 409–412 (2011).
5. Son, M.J. *et al.* Nicotinamide overcomes pluripotency deficits and reprogramming barriers. *Stem Cells* **31**, 1121–1135 (2013).
6. Hong, H. *et al.* Suppression of induced pluripotent stem cell generation by the p53-p21 pathway. *Nature* **460**, 1132–1135 (2009).
7. Utikal, J. *et al.* Immortalization eliminates a roadblock during cellular reprogramming into iPS cells. *Nature* **460**, 1145–1148 (2009).
8. Marión, R.M. *et al.* A p53-mediated DNA damage response limits reprogramming to ensure iPS cell genomic integrity. *Nature* **460**, 1149–1153 (2009).
9. Li, H. *et al.* The Ink4/Arf locus is a barrier for iPS cell reprogramming. *Nature* **460**, 1136–1139 (2009).
10. Li, Y. *et al.* The p53-PUMA axis suppresses iPSC generation. *Nat Commun.* **4**, 2174 (2013).
11. Lake, B.B. *et al.* Context-dependent enhancement of induced pluripotent stem cell reprogramming by silencing Puma. *Stem Cells* **30**, 888–897 (2012).
12. Guo, S. *et al.* Nonstochastic reprogramming from a privileged somatic cell state. *Cell* **156**, 649–662 (2014).
13. Lee, Y.L. *et al.* Sirtuin 1 facilitates generation of induced pluripotent stem cells from mouse embryonic fibroblasts through the miR-34a and p53 pathways. *PLoS ONE* **7**, e45633 (2012).
14. Brosh, R. *et al.* p53 counteracts reprogramming by inhibiting mesenchymal-to-epithelial transition. *Cell Death Differ.* **20**, 312–320 (2013).
15. Ye, D. *et al.* MiR-138 promotes induced pluripotent stem cell generation through the regulation of the p53 signaling. *Stem Cells* **30**, 1645–1654 (2012).
16. Wang, J. *et al.* p53-facilitated miR-199a-3p regulates somatic cell reprogramming. *Stem Cells* **30**, 1405–1413 (2012).
17. Zhu, S. *et al.* Reprogramming of human primary somatic cells by OCT4 and chemical compounds. *Cell Stem Cell* **7**, 651–655 (2010).
18. Silva, J. *et al.* Promotion of reprogramming to ground state pluripotency by signal inhibition. *PLoS Biol.* **6**, e253 (2008).
19. Ichida, J.K. *et al.* A small-molecule inhibitor of Tgf-β signaling replaces *Sox2* in reprogramming by inducing *Nanog*. *Cell Stem Cell* **5**, 491–503 (2009).
20. Hou, P. *et al.* Pluripotent stem cells induced from mouse somatic cells by small-molecule compounds. *Science* **341**, 651–654 (2013).
21. Huangfu, D. *et al.* Induction of pluripotent stem cells by defined factors is greatly improved by small-molecule compounds. *Nat. Biotechnol.* **26**, 795–797 (2008).
22. Federation, A.J., Bradner, J.E. & Meissner, A. The use of small molecules in somatic-cell reprogramming. *Trends Cell Biol.* **24**, 179–187 (2014).
23. Amabile, G. & Meissner, A. Induced pluripotent stem cells: current progress and potential for regenerative medicine. *Trends Mol. Med.* **15**, 59–68 (2009).
24. Eminli, S. *et al.* Differentiation stage determines potential of hematopoietic cells for reprogramming into induced pluripotent stem cells. *Nat. Genet.* **41**, 968–976 (2009).
25. Gurdon, J.B. The developmental capacity of nuclei taken from intestinal epithelium cells of feeding tadpoles. *J. Embryol. Exp. Morphol.* **10**, 622–640 (1962).
26. Li, J., Greco, V., Guasch, G., Fuchs, E. & Mombaerts, P. Mice cloned from skin cells. *Proc. Natl. Acad. Sci. USA* **104**, 2738–2743 (2007).
27. Artavanis-Tsakonas, S. & Muskavitch, M.A. Notch: the past, the present, and the future. *Curr. Top. Dev. Biol.* **92**, 1–29 (2010).
28. Bray, S.J. Notch signalling: a simple pathway becomes complex. *Nat. Rev. Mol. Cell Biol.* **7**, 678–689 (2006).
29. Topley, G.I., Okuyama, R., Gonzales, J.G., Conti, C. & Dotto, G.P. $p21^{WAF1/Cip1}$ functions as a suppressor of malignant skin tumor formation and a determinant of keratinocyte stem-cell potential. *Proc. Natl. Acad. Sci. USA* **96**, 9089–9094 (1999).
30. Missero, C., Di Cunto, F., Kiyokawa, H., Koff, A. & Dotto, G.P. The absence of $p21^{Cip1/WAF1}$ alters keratinocyte growth and differentiation and promotes ras-tumor progression. *Genes Dev.* **10**, 3065–3075 (1996).
31. Aasen, T. & Belmonte, J.C. Isolation and cultivation of human keratinocytes from skin or plucked hair for the generation of induced pluripotent stem cells. *Nat. Protoc.* **5**, 371–382 (2010).
32. Aasen, T. *et al.* Efficient and rapid generation of induced pluripotent stem cells from human keratinocytes. *Nat. Biotechnol.* **26**, 1276–1284 (2008).
33. Blanpain, C., Lowry, W.E., Pasolli, H.A. & Fuchs, E. Canonical notch signaling functions as a commitment switch in the epidermal lineage. *Genes Dev.* **20**, 3022–3035 (2006).
34. Bock, C. *et al.* Reference maps of human ES and iPS cell variation enable high-throughput characterization of pluripotent cell lines. *Cell* **144**, 439–452 (2011).
35. Fuwa, H. *et al.* Divergent synthesis of multifunctional molecular probes to elucidate the enzyme specificity of dipeptidic γ-secretase inhibitors. *ACS Chem. Biol.* **2**, 408–418 (2007).
36. Nam, Y., Sliz, P., Song, L., Aster, J.C. & Blacklow, S.C. Structural basis for cooperativity in recruitment of MAML coactivators to Notch transcription complexes. *Cell* **124**, 973–983 (2006).
37. Nam, Y., Weng, A.P., Aster, J.C. & Blacklow, S.C. Structural requirements for assembly of the CSL.Intracellular Notch1.Mastermind-like 1 transcriptional activation complex. *J. Biol. Chem.* **278**, 21232–21239 (2003).
38. Lefort, K. & Dotto, G.P. Notch signaling in the integrated control of keratinocyte growth/differentiation and tumor suppression. *Semin. Cancer Biol.* **14**, 374–386 (2004).
39. Jones, P.H. & Watt, F.M. Separation of human epidermal stem cells from transit amplifying cells on the basis of differences in integrin function and expression. *Cell* **73**, 713–724 (1993).
40. Kavian, N. *et al.* Targeting ADAM-17/notch signaling abrogates the development of systemic sclerosis in a murine model. *Arthritis Rheum.* **62**, 3477–3487 (2010).
41. Allen, A.S. *et al.* *De novo* mutations in epileptic encephalopathies. *Nature* **501**, 217–221 (2013).
42. Huangfu, D. *et al.* Induction of pluripotent stem cells from primary human fibroblasts with only Oct4 and Sox2. *Nat. Biotechnol.* **26**, 1269–1275 (2008).
43. Mikkelsen, T.S. *et al.* Dissecting direct reprogramming through integrative genomic analysis. *Nature* **454**, 49–55 (2008).
44. Onder, T.T. *et al.* Chromatin-modifying enzymes as modulators of reprogramming. *Nature* **483**, 598–602 (2012).
45. Gore, A. *et al.* Somatic coding mutations in human induced pluripotent stem cells. *Nature* **471**, 63–67 (2011).

Acknowledgments

The authors would like to thank E. Son for assistance with microarray data analysis, S. Sato for assistance with chimera experiments, E. Kiskinis for assistance with nanostring analysis and K. Koszka and M. Yamaki for assistance with teratoma experiments. The authors are grateful for the financial support that made this work possible. K.E. was supported by US National Institutes of Health (NIH)

R01 grant 5R01GM096067, NIH P01 grant 5P01GM099117 and the Howard Hughes Medical Institute. A.M. was supported by NIH P01 grant 5P01GM099117. H.A. was supported by grants from the Ministry of Education, Culture, Sports, Science and Technology (MEXT) of Japan, Grant-in-aid for Scientific Research (21390456) and Grant-in-Aid for challenging Exploratory Research (22659304) and a grant from JST-CREST. J.K.I. was supported by a Stan and Fiona Druckenmiller-New York Stem Cell Foundation postdoctoral fellowship, NIH K99 grant 1K99NS077435-01A1, NIH R00 grant 4R00NS077435-03 and the Novartis Institutes for BioMedical Research. C.B. was supported by a Feodor Lynen Fellowship from the Alexander von Humboldt Foundation.

Author contributions

A.M. and J.E.B. hypothesized that Notch inhibition might aid reprogramming. J.K.I., J.T., A.M., A.U., L.L.R. and K.E. designed reprogramming and mechanistic experiments to test the hypothesis. J.K.I., J.T., A.C.C., L.A.W., Y.S., M.T.M., S.S., G.A. and H.A. performed reprogramming experiments and characterization of the iPSCs. C.B. and M.Z. performed bioinformatic analysis of transcriptional data characterizing the iPSCs. J.K.I., J.T., A.C.C. and Y.S. performed experiments to determine the mechanism of action of DAPT and Notch inhibition in reprogramming. K.E., J.K.I. and J.T. discovered and confirmed the mechanism of action of DAPT. K.E. and J.K.I. wrote the paper. All authors helped in paper revision.

Competing financial interests

The authors declare no competing financial interests.

Additional information

Supplementary information is available in the online version of the paper. Reprints and permissions information is available online at http://www.nature.com/reprints/index.html. Correspondence and requests for materials should be addressed to H.A., A.M. or K.E.

ONLINE METHODS

iPSC reprogramming experiments. The IACUC committee of Harvard University approved the use of mice for all experiments included in this paper. *Oct4*:GFP neonatal mouse keratinocytes were isolated from P1-P2 pups using an overnight digestion in either 0.25% trypsin/EDTA or TrypLE (Life Technologies) at 4 °C. They were cultured in SFM medium (Life Technologies) on collagen IV–coated plates. Neonatal human epidermal keratinocytes (Lonza) were cultured in Epilife medium (Invitrogen) on collagen-coated plates. Keratinocytes were reprogrammed using retroviruses containing either mouse or human *OCT4*, *SOX2*, *KLF4* and *CMYC* produced in the pMXs backbone. Chemical treatment was initiated 1–2 d after viral transduction and readministered every other day until the end of the experiment unless otherwise specified. DAPT (EMD Millipore) was used at 10 μM for reprogramming experiments using *OCT4*, *SOX2*, *KLF4* and *CMYC* and 2.5 μM for *OCT4*, *SOX2* reprogramming experiments unless otherwise noted. DBZ was used at 2 μM. Irradiated mouse embryonic fibroblast feeders were added 6 d after transduction, and the medium was changed to mouse or human embryonic stem cell medium at that time. Colonies were scored as iPSC colonies if they were *Oct4*::GFP+ in mouse experiments or NANOG+/TRA-1-81+ in human experiments.

Gene expression analysis of iPSCs. Nanostring (Nanostring Technologies) and scorecard analysis was performed as described[34]. iPSCs were cultured in mTesr1 medium (Stem Cell Technologies) before RNA isolation. To measure their differentiation propensities, iPSCs were dissociated into embryoid bodies and cultured in human embryonic stem cell medium without bFGF for 16 d. Cells were then lysed, and total RNA was extracted using Trizol (Life Technologies) and purified using the RNeasy kit (QIAGEN). 300–500 ng of RNA was profiled on the Nano-String nCounter system (Nanostring Technologies) according to the manufacturer's instructions. A custom nCounter codeset covering 500 genes that monitor cell state, pluripotency and differentiation was used[34]. Data analysis was performed with the R statistics package as in ref. 34. Briefly, the lineage scorecard performs a parametric gene set enrichment analysis on *t* scores obtained from a pairwise comparison between the cell line of interest and the reference of ES cell–derived EBs.

Differentiation of iPSCs. For teratoma formation, 1–2 million human iPSCs were injected into the kidney capsule of nude mice and harvested 2 months later. Teratomas were sectioned and stained with hematoxylin and eosin for visualization. For the mouse iPSC chimera assay, 10 *Oct4*::GFP+ iPSCs were injected per ICR blastocyst, and 20 blastocysts were transplanted into each pseudopregnant female. Embryos were either allowed to develop to term or harvested at day E12.5 and dissected for genital ridge analysis using a stereomicroscope.

Gene expression analysis of reprogramming cultures. Illumina MouseRef-8 microarrays (Illumina) were used for genome-wide mRNA expression analysis of reprogramming mouse keratinocyte cultures treated with DMSO or 10 μM DAPT. For qPCR analysis, RNA was isolated using Trizol, cDNA synthesis was performed using the iScript cDNA synthesis kit (Bio-Rad), and the SYBR Green qPCR Supermix (Bio-Rad) was used for PCR product detection.

Western blots and immunofluorescence. Antibodies detecting mouse Notch (Santa Cruz Biotechnology, sc-6015, 1:1,000), human NOTCH (Abcam, ab27526, 1:1,000 and Santa Cruz Biotechnology, sc-23307, 1:1,000), cleaved human NOTCH (Cell Signaling Technology, 2421, 1:1,000), p53 (Santa Cruz Biotechnology, sc-56182, 1:1,000), Involucrin (Abcam, Ab53112) and p21 (Cell Signaling Technology 05-345, 1:1,000) were used for western blots. Blots were quantified using ImageJ software. Antibodies specific for NANOG (Abcam, AF1997, 1:400) and TRA-1-81 (Chemicon, MAB4381, 1:500) were used to identify human iPSCs. A γH2AX (Abcam, ab11175, 1:400) antibody was used to detect γH2AX foci. Cells in which γH2AX staining covered greater than half the nucleus were scored as positive for γH2AX foci.

UV irradiation assay. UV irradiation was performed at a dosage of 30 J. TUNEL staining was performed using a TUNEL kit (Pharmacia Biosciences).

shRNA and siRNA knockdown experiments. shRNAs and siRNAs were purchased from Sigma and added to reprogramming cultures within 1 d after addition of the reprogramming retroviruses. shRNAs (TRCN0000003753, p53 and TRCN0000287021, p21) were expressed in the pLKO.1 lentiviral backbone. siRNAs were used at 80 nM and were transfected into reprogramming cultures using RNAiMAX (Life Technologies).

Array CGH analysis of iPSC lines. Cell Line Genetics performed array CGH analysis of iPSC lines at passage 5 using 4x180K+SNP analysis.

Statistical analysis. For all experiments, error bars represent the s.d. between two or three biological replicates, and statistical significance was determined using a two-tailed homoscedastic Student's *t*-test.

doi:10.1038/nchembio.1552

ERRATUM

Notch inhibition allows oncogene independent generation of iPS cells

Justin K Ichida, Julia T C W, Luis A Williams, Ava C Carter, Yingxiao Shi, Marcelo T Moura, Michael Ziller, Sean Singh, Giovanni Amabile, Christoph Bock, Akihiro Umezawa, Lee L Rubin, James E Bradner, Hidenori Akutsu, Alexander Meissner & Kevin Eggan

Nat. Chem. Biol. **10**, 632–639 (2014); published online 22 June 2014; corrected after print 29 July 2014.

In the version of this article initially published, Julia TCW's name was misspelled as Julia T C W. In addition, her initials in the author contribution statement should have read J.T. instead of J.T.C.W. The error has been corrected in the HTML and PDF versions of the article.

ERRATUM

Notch inhibition allows oncogene-independent generation of iPS cells.

Justin K Ichida, Julia T C W, Luis A Williams, Ava C Carter, Yingxiao Shi, Marcelo T Moura, Michael Ziller, Sean Singh, Giovanni Amabile, Christoph Bock, Akihiro Umezawa, Lee L Rubin, James E Bradner, Hidenori Akutsu, Alexander Meissner & Kevin Eggan

Nat. Chem. Biol. **10**, 632–639 (2014); published online 22 June 2014; corrected after print 29 July 2014 and 14 August 2014

In the version of this article initially published, a black bar was erroneously placed in the scrambled shRNA column in Figure 3g. The error has been corrected for the PDF and HTML versions of the article.

OPEN ACCESS Freely available online

PLOS | ONE

A Novel *In Vitro* Method for Detecting Undifferentiated Human Pluripotent Stem Cells as Impurities in Cell Therapy Products Using a Highly Efficient Culture System

Keiko Tano[1,2], Satoshi Yasuda[2], Takuya Kuroda[2], Hirohisa Saito[3], Akihiro Umezawa[1], Yoji Sato[2,4,5,6]*

1 Department of Reproductive Biology, National Research Institute for Child Health and Development, Tokyo, Japan, **2** Division of Cellular & Gene Therapy Products, National Institute of Health Sciences, Tokyo, Japan, **3** National Research Institute for Child Health and Development, Tokyo, Japan, **4** Department of Quality Assurance Science for Pharmaceuticals, Graduate School of Pharmaceutical Sciences, Nagoya City University, Aichi, Japan, **5** Department of Cellular & Gene Therapy Products, Graduate School of Pharmaceutical Sciences, Osaka University, Osaka, Japan, **6** Department of Translational Pharmaceutical Sciences, Graduated School of Pharmaceutical Sciences, Kyushu University, Fukuoka, Japan

Abstract

Innovative applications of cell therapy products (CTPs) derived from human pluripotent stem cells (hPSCs) in regenerative medicine are currently being developed. The presence of residual undifferentiated hPSCs in CTPs is a quality concern associated with tumorigencity. However, no simple *in vitro* method for direct detection of undifferentiated hPSCs that contaminate CTPs has been developed. Here, we show a novel approach for direct and sensitive detection of a trace amount of undifferentiated human induced pluripotent stem cells (hiPSCs) using a highly efficient amplification method in combination with laminin-521 and Essential 8 medium. Essential 8 medium better facilitated the growth of hiPSCs dissociated into single cells on laminin-521 than in mTeSR1 medium. hiPSCs cultured on laminin-521 in Essential 8 medium were maintained in an undifferentiated state and they maintained the ability to differentiate into various cell types. Essential 8 medium allowed robust hiPSC proliferation plated on laminin-521 at low cell density, whereas mTeSR1 did not enhance the cell growth. The highly efficient culture system using laminin-521 and Essential 8 medium detected hiPSCs spiked into primary human mesenchymal stem cells (hMSCs) or human neurons at the ratio of 0.001%–0.01% as formed colonies. Moreover, this assay method was demonstrated to detect residual undifferentiated hiPSCs in cell preparations during the process of hMSC differentiation from hiPSCs. These results indicate that our highly efficient amplification system using a combination of laminin-521 and Essential 8 medium is able to detect a trace amount of undifferentiated hPSCs contained as impurities in CTPs and would contribute to quality assessment of hPSC-derived CTPs during the manufacturing process.

Citation: Tano K, Yasuda S, Kuroda T, Saito H, Umezawa A, et al. (2014) A Novel *In Vitro* Method for Detecting Undifferentiated Human Pluripotent Stem Cells as Impurities in Cell Therapy Products Using a Highly Efficient Culture System. PLoS ONE 9(10): e110496. doi:10.1371/journal.pone.0110496

Editor: Graca Almeida-Porada, Wake Forest Institute for Regenerative Medicine, United States of America

Received March 28, 2014; **Accepted** September 16, 2014; **Published** October 27, 2014

Data Availability: The authors confirm that all data underlying the findings are fully available without restriction. All relevant data are within the paper and its Supporting Information files.

Funding: This work was supported by Research Grants from the Japanese Ministry of Health, Labour and Welfare (H23-SAISEI-IPPAN-004, H23-SAISEI-IPPAN-005, H24-IYAKU-SHITEI-027, H25-JITSUYOKA(SAISEI)-IPPAN-008, and Marketing Authorization Facilitation Program for Innovative Therapeutic Products), http://www.mhlw.go.jp/english/policy/other/research-projects/index.html. The funders had no role in study design, data collection and analysis, decision to publish, or preparation of the manuscript.

Competing Interests: The authors have declared that no competing interests exist.

* Email: yoji@nihs.go.jp

Introduction

Cell therapy products (CTPs) are expected to offer promising treatments for serious and life-threating diseases for which no adequate therapy is currently available. An increasing number of CTPs derived from human pluripotent stem cells (hPSCs), i.e. induced pluripotent stem cells (hiPSCs) and embryonic stem cells (hESCs), are being developed for regenerative medicine/cell therapy because of their infinite self-renewal capacity and their ability to differentiate into various types of cells. Quality assessment of CTPs is critical to ensure their safety and efficacy for clinical application [1]. CTPs derived from hPSCs possibly include the cells of interest and also other cells such as undifferentiated cells, precursor cells and other differentiated cells. The presence of residual undifferentiated cells in CTPs derived from hPSCs is one of the most serious concerns for tumorigenicity because the undifferentiated hPSCs have a capacity to form teratoma in animals [1–4]. Hentze et al. previously reported that hundreds of undifferentiated hESCs were enough to produce a teratoma in immunodeficient SCID mice [5]. We cannot exclude the possibility that a trace amount of residual undifferentiated hPSCs in CTPs cause ectopic tissue formation, tumor development and/or malignant transformation after transplantation. Therefore, establishment of a detection method for residual undifferentiated cells is necessary for the safety and quality assessment of CTPs derived from hPSCs.

An *in vivo* teratoma formation assay is the only method to directly assess tumorigenicity of undifferentiated cells, but this assay is costly and time-consuming [2,3]. Several *in vitro* methods, such as flow cytometry and quantitative real-time PCR (qRT-PCR) analysis, can also detect residual undifferentiated hPSCs in CTPs [2,3]. Our previous report has shown that flow cytometry

using anti-TRA-1-60 antibody and qRT-PCR using a specific probe and primers for *LIN28* mRNA can detect as low as 0.1% and 0.002% undifferentiated hiPSCs spiked into retinal pigment epithelial (RPE) cells, respectively [3]. However, both of these methods have the disadvantage of detecting undifferentiated cell marker expression but not functionally undifferentiated cells *per se*. The soft agar colony formation assay is commonly used to detect tumorigenic cells with a property of anchorage-independent growth. However, this assay is not appropriate for the detection of hPSCs because they undergo apoptosis associated with dissociation into single cells [3,6]. At present, there is no simple method to directly detect a trace amount of hPSCs *in vitro*.

Recently, some cell culture matrices have been reported to sustain self-renewal of dissociated hPSCs without apoptosis [7,8]. We focused on a culture system enabling hPSC cell growth without apoptosis and developed a direct *in vitro* method for detecting a trace amount of undifferentiated hPSCs in CTPs. Laminin-521, a laminin isoform that is normally expressed in hESCs, is known to stimulate robust hPSC proliferation in an undifferentiated state in combination with mTeSR1 medium [7]. In the present study, we present a novel approach to detect undifferentiated hiPSCs contaminating CTPs through efficient amplification using a laminin-521-based cell culture system with Essential 8 medium [9] instead of mTeSR1 medium.

Materials and Methods

Cell culture

The hiPSC lines, 201B7, 253G1 and 409B2, were provided by the RIKEN BRC through the Project for Realization of Regenerative Medicine and the National Bio-Resource Project of the MEXT, Japan [17–19]. hiPSCs were first cultured on mitomycin C-treated SNL cells (a mouse fibroblast STO cell line expressing a neomycin-resistance gene cassette and LIF) in primate ES cell medium (ReproCell, Kanagawa, Japan) supplemented with 4 ng/ml human basic fibroblast growth factor (bFGF; R&D Systems, Inc., Minneapolis, USA). hiPSC colonies were passaged as small clumps once every 5–6 days using CTK solution (ReproCell) and STEMPRO EZPassage (Invitrogen, Carlsbad, CA, USA). hiPSCs were then passaged onto Matrigel-coated dishes with mTeSR1 (Stem Cell Technologies, Vancouver, CAN) for at least 2 passages before plating on laminin-521 or directly subcultured onto laminin-521-coated dishes. Subculture on laminin-521-coated dishes was performed as follows: near-confluent cells were treated with 0.5 mM EDTA/D-PBS for 6–7 minutes at 37°C. Cells were pipetted to achieve single-cell suspension and centrifuged at 30× *g* for 4 minutes. After centrifugation, the cell pellet was suspended in Essential 8 medium (Life Technologies, USA) and seeded at $2-3\times10^4$ cells/cm^2 on laminin-521-coated dishes. Cells were grown in Essential 8 medium at 37°C in a 5% CO_2 atmosphere and passaged once in 3–4 days. Primary human mesenchymal stem cells (hMSCs) were purchased from Lonza and cultured in MSCGM medium (Lonza, Walkersville, MO, USA). hMSCs at passage 7 were used in this study. Primary human neurons were purchased from ScienCell Research Laboratories (Carlsbad, CA, USA).

Cell proliferation assay

hiPSCs were dissociated into single cells and seeded on matrix-coated plates at a density of 3×10^4 cells/cm^2 or at the indicated density as described below. Tissue culture plates (BD Falcon, NJ, USA) were coated with laminin-521 (BioLamina, Sundbyberg, Sweden) dissolved in D-PBS at 4 μg/cm^2 at 37°C for 2 h. Control plates were coated with Matrigel (BD Biosciences, MA, USA) at 16 μg/cm^2. Viable cells were quantified every 24 h using CyQUANT Cell Proliferation Assay Kit (Life Technologies) according to the manufacturer's instructions.

Quantitative RT-PCR

Total RNA was treated with DNase I and isolated using RNeasy Mini Kit (Qiagen Hilden, Germany) according to the manufacturer's instructions. Quantitative RT-PCR was performed using the QuantiTect Probe one-step RT-PCR Kit (Qiagen) on StepOnePlus Real Time PCR system (Life Technologies). Gene expression levels were normalized to *GAPDH* expression levels, which were quantified using TaqMan human GAPDH control reagents (Life Technologies). Primers and probes were obtained from Sigma-Aldrich. The sequences of primers and probes are listed in Table S1.

Teratoma assay

Teratoma formation experiments were performed by injecting 253G1 cells (1×10^6 cells/testis) that were cultured with laminin-521 and Essential 8 medium (passage 36), into the testes of severe combined immunodeficiency (SCID) mice at the age of 8 weeks under pentobarbital anesthesia. The mice were sacrificed with an overdose of pentobarbital 10 weeks after the transplant, and the isolated teratoma was fixed in 10% formalin. The paraffin-embedded section was stained with hematoxylin and eosin (HE). Animal experiments were performed at UNITECH Co., Ltd. (Chiba, Japan) in accordance with the animal ethical committee's approval (Permit Number: KIS-130712i-20 at UNITECH Co., Ltd. and 444 at NIHS).

Differentiation assay

Differentiation of hiPSCs into three germ layers was performed as follows: 253G1 cells were plated on laminin-521 at a density of 3×10^4 cells/cm^2 in Essential 8 medium and expanded until they were nearly confluent. A) Ectoderm lineage differentiation: Neural hiPSCs differentiation was performed according to the previously reported protocol with some modifications [10]. Briefly, culture medium was changed from Essential 8 to DMEM/F12 medium containing 20% knockout serum replacement (KSR, Life Technologies), 10 μM SB431542 (Sigma-Aldrich) and 500 ng/ml Noggin (R&D systems). After 4 days of differentiation, SB431542 was withdrawn and increasing amounts of N2 medium (25%, 50%, or 75%) was added to the KSR medium every 2 days. From day 10 of differentiation, the medium was changed to N2B27 medium without bFGF containing 500 ng/ml Noggin, and cells were cultured for 15 days. B) Mesoderm lineage differentiation: hiPSCs were cultured for 15 days in DMEM/F12 containing 10% FBS, 2 mM L-glutamine 1% nonessential amino acids (Life Technologies) and 0.1 mM β-mercaptoethanol [8]. C) Endoderm lineage differentiation: hepatic differentiation of hiPSCs was performed according to the previously reported protocol with some modifications [11]. On the first day of differentiation, the medium was replaced with RPMI1640 (Sigma-Aldrich) containing B27 supplement (Life Technologies), 100 ng/ml activin A (R&D systems), 50 ng/ml Wnt3a (R&D systems) and 1 mM sodium butyrate (NaB) (Sigma-Aldrich). On the following 2 days, NaB was omitted from the medium. After 3 days of differentiation, the medium was replaced with knockout-DMEM containing 20% KSR, 1 mM L-glutamine, 1% nonessential amino acids, and 1% DMSO for 5 days.

Differentiation of 253G1 cells into MSCs was performed according to the previously reported protocol with some modifications [14]. On the first day of differentiation, 253G1 cells

subcultured on laminin-521 in Essential 8 medium were dissociated into single cells and suspended in EB formation medium (AggreWell Medium, Stem Cell Technologies) with 10 μM Y-27632 (Wako, Japan), a ROCK inhibitor for generation of embryoid bodies (EBs). Cells (1×10^6) were then added to a well of the AggreWell Plate and incubated for 24 h at 37°C in a 5% CO_2 atmosphere. After 24 h, EBs were plated on 35-mm dishes (BD) in Stemline II (Sigma-Aldrich) supplemented with 50 ng/ml BMP4 (R&D systems) and 50 ng/ml VEGF (R&D systems) for 2 days. Medium was changed to Stemline II containing BMP4 (50 ng/ml), VEGF (50 ng/ml) and bFGF (22.5 ng/ml), and the EBs were cultured for 2 days. EBs were dissociated into single cells and replated in Methocult H4536 (Stem Cell Technologies) containing Growth Enhancement Media Supplement (EX-CYTE, Millipore), 50 ng/ml VEGF, 50 ng/ml Flt3-ligand (R&D systems), 50 ng/ml thrombopoietin (R&D systems) and 30 ng/ml bFGF for hemangioblast formation. After 8 days, cultures were harvested and plated as defined passage 0 in MSC growth medium (αMEM+ 20% FBS) on Matrigel.

Immunofluorescence staining

Immunofluorescence staining was performed as follows: cells were fixed with 4% paraformaldehyde in PBS for 15 minutes. After washing three times with PBS, cells were permeabilized with 0.1% Triton X-100 in PBS for 10 minutes, and then blocked with Blocking One (nacalai tesque, Kyoto, Japan) at 4°C over night. Cells were incubated with primary antibody against α-fetoprotein (AFP, 1:400; Dako) for 30 minutes at room temperature, with antibody against smooth muscle actin (SMA, 1:400; Sigma-Aldrich), βIII tubulin (0.5 μg/ml; abcam) or TRA-1-60 (1:200; Millipore) for 1 hour at room temperature, or with antibody against CD105 (1:200; abcam) at 4°C over night. After washing with PBS three times, cells were incubated with secondary antibody conjugated with Alexa Fluor 488 (Invitrogen) for 30 minutes at RT. VECTASHIELD mounting medium with DAPI (VECTOR) was used for nuclear staining. The samples were examined using an Olympus IX71 microscope equipped with cellSens Standard software (Olympus).

Embryoid body formation

Embryoid bodies were generated from hiPSCs using AggreWell 800 plates (Stem Cell Technologies) according to the manufacturer's instructions, with some modifications. hiPSCs dissociated with 0.5 mM EDTA were collected and suspended in EB formation medium (AggreWell Medium, Stem Cell Technologies) supplemented with 10 μM Y-27632 (Wako). The cells were added to each well (5×10^5 cells/well) in the AggreWell plate and incubated for 24 h at 37°C in a 5% CO_2 atmosphere. EBs were harvested from AggreWell plate and cultured in 35-mm dishes (BD) with primate ES cell culture medium (ReproCell) without bFGF. The medium was changed every 3 days. After 10 days of incubation, total RNA was isolated from EBs. The expression levels of each differentiation marker were determined using quantitative RT-PCR, as described above.

Statistics

Statistical analysis was performed using SigmaPlot 12.5 Software (Systat Software Inc., CA). The data were analyzed using two-way ANOVA or two-way repeated-measures ANOVA followed by a Bonferroni t-test as a post hoc test. A probability below 0.05 was considered significant.

Results

Essential 8 medium promotes hiPSCs cell growth on laminin-521

hPSCs are known to easily undergo apoptosis induced by dissociation [6]. To achieve an efficient hPSC cell growth, we determined the optimal culture conditions that allow robust proliferation of hiPSCs dissociated into single cells. Here, we focused on laminin-521 as a cell culture matrix, which permits survival of dissociated hPSCs without a Rho-associated protein kinase (ROCK) inhibitor [7]. mTeSR1 medium is conventionally used to culture dissociated hiPSCs on dishes coated with laminin-521 [7], and other hPSC media besides mTeSR1 have not been fully characterized with laminin-521. To examine effects of medium on hPSC cell growth on laminin-521, we compared the hiPSC growth rate using conventional mTeSR1 medium with Essential 8 medium, with optimized components [9]. After subculture on Matrigel, 253G1 hiPSCs were dissociated into single cells and seeded on laminin-521-coated plates at a density of 3×10^4 cells/cm^2. No difference was observed between mTeSR1 and Essential 8 medium in the cell number of hiPSCs cultured on laminin-521 at 24 h after plating (Figure 1A and 1B). However, the cells cultured on laminin-521 in Essential 8 medium showed rapid expansion compared to those in the mTeSR1 medium, and they reached nearly confluent at 72 h after plating (Figure 1A). Cell growth quantification revealed that the number of cells in Essential 8 medium was 3-fold higher than those in mTeSR1 medium at 72 h after plating (Figure 1B). Similar results were also obtained using another hiPSC line, 201B7 (Figure S1A). These results suggest that Essential 8 medium promotes hiPSC proliferation more rapidly than mTeSR1 medium when grown on laminin-521. When dissociated hiPSCs were cultured on Matrigel, Essential 8 medium did not significantly promote cell proliferation compared with mTeSR1 medium (Figure 1B and Figure S1A). We found that Essential 8 medium enhanced the hiPSC growth rate even on LM511-E8, which is a fragment of laminin 511 [8], but this effect was weaker than that on laminin-521 (Figure S1B). Taken together, these results suggest that a combination of laminin-521 and Essential 8 medium is a potent cell culture system for efficient amplification of dissociated hiPSCs *in vitro* compared to other culture systems. Therefore, we decided to develop a novel method for detecting undifferentiated hPSCs using a combination of laminin-521 and Essential 8 medium.

Culture system using laminin-521 and Essential 8 medium maintains the undifferentiated state and pluripotency of hiPSCs

We next examined whether a culture system using laminin-521 and Essential 8 medium maintains undifferentiated states through serial passages. 253G1 cells were dissociated into single cells and sequentially subcultured on laminin-521 in Essential 8 medium. 253G1 cells exhibited vigorous proliferation for more than 30 passages under these conditions (data not shown). Quantitative RT-PCR analysis revealed that the expression levels of undifferentiated hPSC markers (*OCT3/4*, *NANOG*, *SOX2* and *LIN28*) in 253G1 cells cultured with laminin-521 and Essential 8 medium were similar to those cultured with Matrigel and mTeSR1 medium (Figure 2A). Moreover, the serial passages with laminin-521 and Essential 8 medium did not have any effect on expression of the undifferentiated markers. We also examined the effects of subculture on laminin-521 in Essential 8 medium using other hiPSC lines, 201B7 and 409B2, and showed that these cells expressed undifferentiated markers through serial passages (Figure S2A-B). We next tested the pluripotency of hiPSCs cultured on laminin-521 in Essential 8 medium using lineage-specific

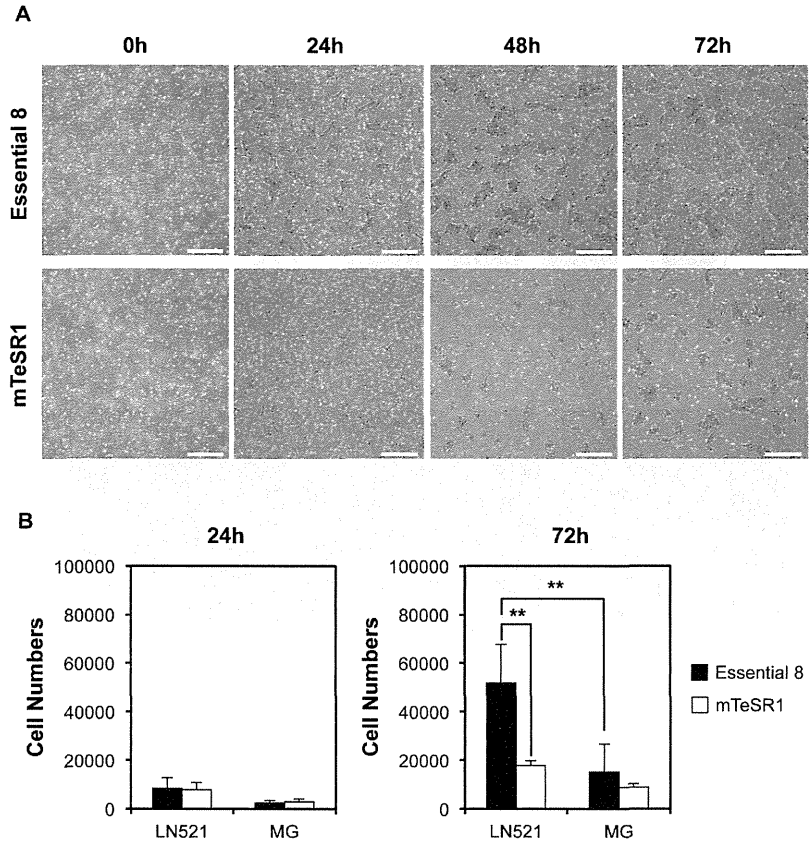

Figure 1. Robust proliferation of 253G1 cells cultured on laminin-521 in Essential 8 medium. (A) Morphology of the 253G1 cells expanded on laminin-521 in Essential 8 or mTeSR1 medium after dissociation into single cells. Scale bars, 500 μm. (B) Quantification of the number of dissociated 253G1 cells expanded on laminin-521 or Matrigel in Essential 8 or mTeSR1 medium. Data are presented as the mean ± standard deviation (SD) of three independent experiments (**$P<0.01$, two-way ANOVA followed by Bonferroni t-test as post-hoc test). LN521, laminin-521; MG, Matrigel.
doi:10.1371/journal.pone.0110496.g001

differentiation protocols. Immunofluorescence analysis using antibodies specific for markers of three germ layers clearly demonstrated that 253G1 cells subcultured with laminin-521 and Essential 8 medium could selectively differentiate into endoderm, mesoderm and ectoderm expressing AFP, α-SMA and βIII tubulin, respectively (Figure 2B). To further examine pluripotency of hiPSCs subcultured with laminin-521 and Essential 8 medium, we facilitated spontaneous differentiation of cells grown as aggregates (embryoid bodies). Embryoid bodies derived from 253G1 cells increased gene expression of differentiated markers for all three germ layer lineages (Figure 2C), consistent with the observation obtained using 201B7 and 409B2 cells (Figure S2C-D). We also confirmed that 253G1 cells cultured with laminin-521 and Essential 8 medium were engrafted in testes of SCID mice and formed teratomas that involved all three germ layers (Figure 2D). These results strongly suggest that a culture system using laminin-521 and Essential 8 medium supports the undifferentiated state and pluripotency of hiPSCs through serial passages.

Essential 8 medium enables hiPSCs to proliferate rapidly from low cell density on laminin-521

Higher sensitivity is expected to ensure the accuracy and reliability of the detection of trace amounts of undifferentiated cells. To achieve higher sensitivity, culture system using laminin-521 and Essential 8 should have a capacity to rapidly expand hPSCs even at a low cell density. Therefore, we next tested whether Essential 8 medium promotes expansion of the hiPSCs on laminin-521 plated at a low cell density. 253G1 cells were seeded into laminin-521-coated plates at a density of 3.2×10^4 cells/cm^2, 1.6×10^4 cells/cm^2 and 8.0×10^3 cells/cm^2, and grown until nearly confluent. Cells grown in mTeSR1 reduced proliferative capacity as seeding density became lower. Conversely, cells cultured in Essential 8 medium showed robust propagation over a prolonged period of time even when they were seeded at low cell density (Figure 3A-C). Similarly, 201B7 and 409B2 cells seeded at lower density in Essential 8 medium also showed robust proliferation compared to the cells in mTeSR1 (Figure 3D-I). Essential 8 medium also promoted cell growth when hiPSCs were plated at lower density of 800 cells/cm^2 (Figure S3). These results indicate that Essential 8 medium promotes expansion of hiPSCs plated on laminin-521 at a low cell density. Thus, a culture system using laminin-521 and Essential 8 medium is considered to be well suited for direct detection of trace amounts of undifferentiated cells.

Culture system using laminin-521 and Essential 8 medium is useful for direct detection of undifferentiated hiPSCs contained in somatic cells

Residual undifferentiated cells contaminating hPSC-based CTPs are a quality concern associated with tumorigencity [1–4].

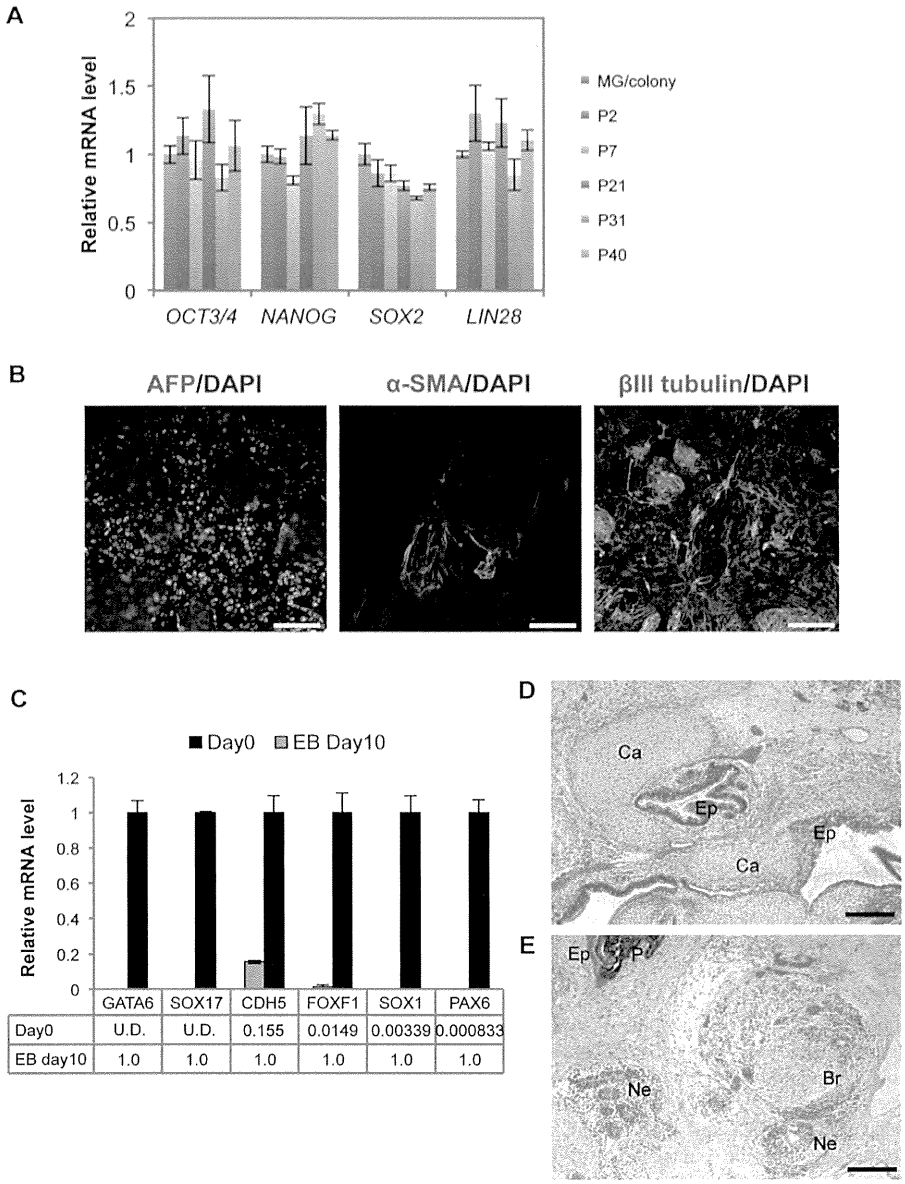

	GATA6	SOX17	CDH5	FOXF1	SOX1	PAX6
Day0	U.D.	U.D.	0.155	0.0149	0.00339	0.000833
EB day10	1.0	1.0	1.0	1.0	1.0	1.0

Figure 2. Characterization of 253G1 cells subcultured on laminin-521 in Essential 8 medium. (A) Expression levels of undifferentiated cell markers (*OCT3/4, NANOG, SOX2 and LIN28*) in 253G1 cells subcultured on laminin-521 in Essential 8 were determined using qRT-PCR. Relative mRNA expression levels are presented as ratios to the level of that in control cells on Matrigel. Results are the mean ± SD (n = 3). (B) *In vitro* differentiation analysis of 253G1 cells subcultured on laminin-521 in Essential 8 medium. Immunostaining of the markers for three germ layers are shown: endoderm (alpha-fetoprotein (AFP)), mesoderm (α-smooth muscle actin (SMA)) and ectoderm (βIII tubulin). Scale bars, 200 μm. (C) Expression levels of differentiated cell markers in embryoid bodies (EBs) derived from 253G1 cells: endoderm (*GATA6, SOX17*), mesoderm (*CDH5, FOXF1*), ectoderm (*SOX1, PAX6*). Relative mRNA expression levels are presented as ratios to the level of that in control cells (EBs at Day 10). Results are the mean ± SD (n = 3). (D-E) Teratomas derived from 253G1 cells cultured on laminin-521 in Essential 8 medium are shown. Hematoxylin and eosin staining showed the features of three germ layers: Ep, epithelium-like tissue (endoderm); Ca, cartilage (mesoderm); Ne, neural rosette-like tissue (ectoderm); P, pigmented neuroectodermal resembling meranocyte (ectoderm); Br, brain-like tissue (ectoderm). Scale bars, 200 μm.
doi:10.1371/journal.pone.0110496.g002

To determine whether a culture system using laminin-521 and Essential 8 medium can detect a trace amount of undifferentiated hiPSCs in CTPs, we spiked dissociated hiPSCs into primary human somatic cells and cultured these cells on laminin-521 in Essential 8 medium. As a model of the somatic cells, we employed human mesenchymal stem cells (hMSCs), because "off-the-shelf" hMSCs derived from hPSCs are a promising CTP [12–14]. We spiked 409B2 cells (1%, 1000 cells; 0.1%, 100 cells; 0.01%, 10 cells) into 1×10^5 hMSCs and plated these cells onto laminin-521-coated wells. hiPSCs were co-cultured with hMSCs on laminin-521-coated dishes in Essential 8 medium and formed distinctive colonies (Figure 4A). At day 7 after plating, we detected 362, 42.5 and 6 colonies (the mean of duplicate measurements) in 1%, 0.1% and 0.01% spiked samples, respectively (Figure 4B). We did not

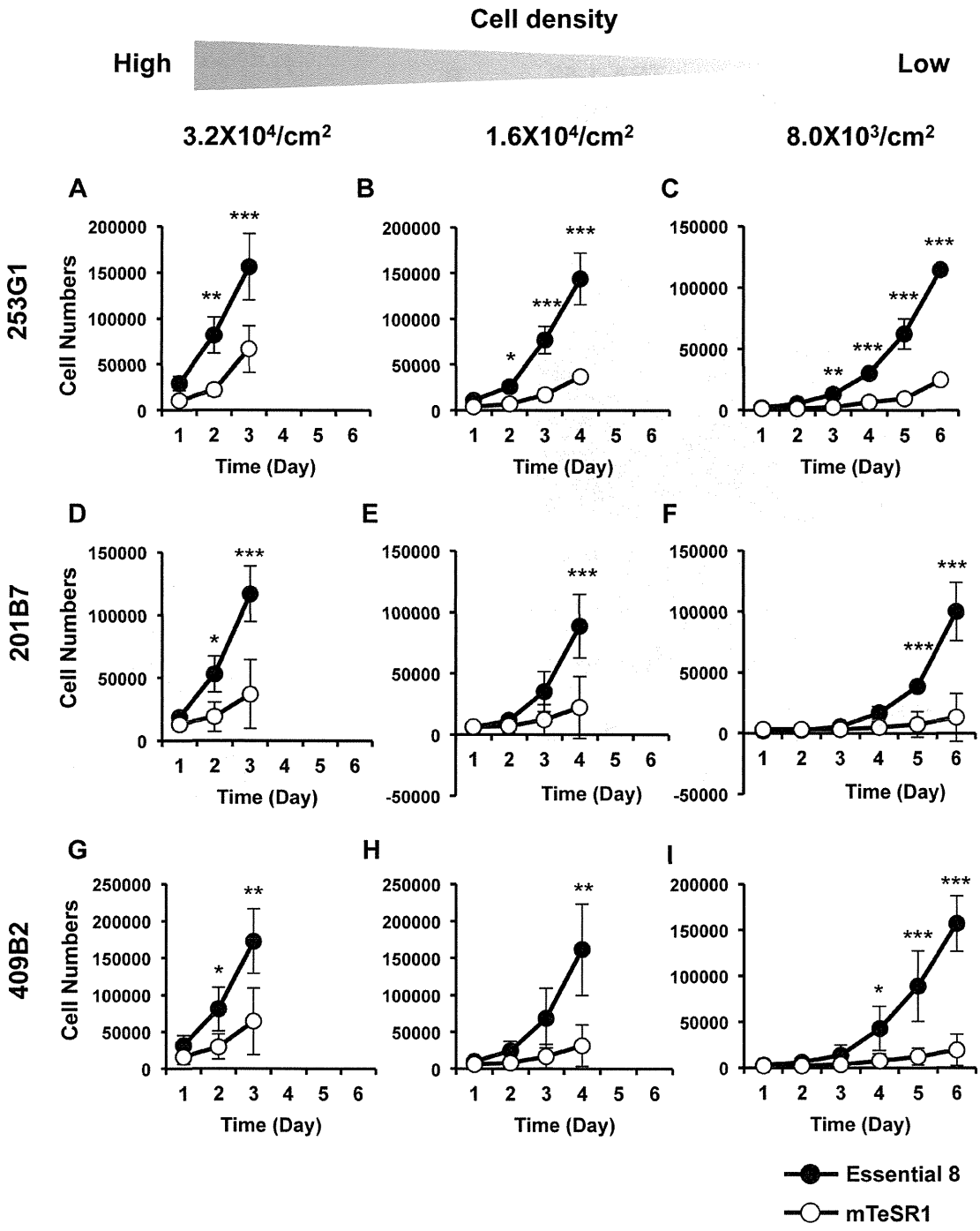

Figure 3. Rapid cell proliferation of hiPSCs plated at low cell density on laminin-521 in Essential 8 medium. (A-I) Quantification of the number of 253G1, 201B7 and 409B2 cells expanded on laminin-521 in Essential 8 or mTeSR1 medium. Cell numbers were counted every 24 h after plating at 3.2×10^4 cells/cm^2 (A, D, G), 1.6×10^4 cells/cm^2 (B, E, H) and 8.0×10^3 cells/cm^2 (C, F, I), respectively. Data are presented as the mean ± standard deviation (SD) of three independent experiments (*$P<0.05$, **$P<0.01$, *** $P<0.001$, two-way repeated-measures ANOVA followed by a Bonferroni post-hoc test).
doi:10.1371/journal.pone.0110496.g003

find any colonies when only hMSCs were cultured on laminin-521 in Essential 8 medium. In addition, immunofluorescence staining with anti-TRA-1-60 antibody showed that these colonies formed in an undifferentiated state (Figure 4A), suggesting that colonies derived from hiPSCs were formed in an hMSC monolayer under conditions with laminin-521 and Essential 8 medium. We also

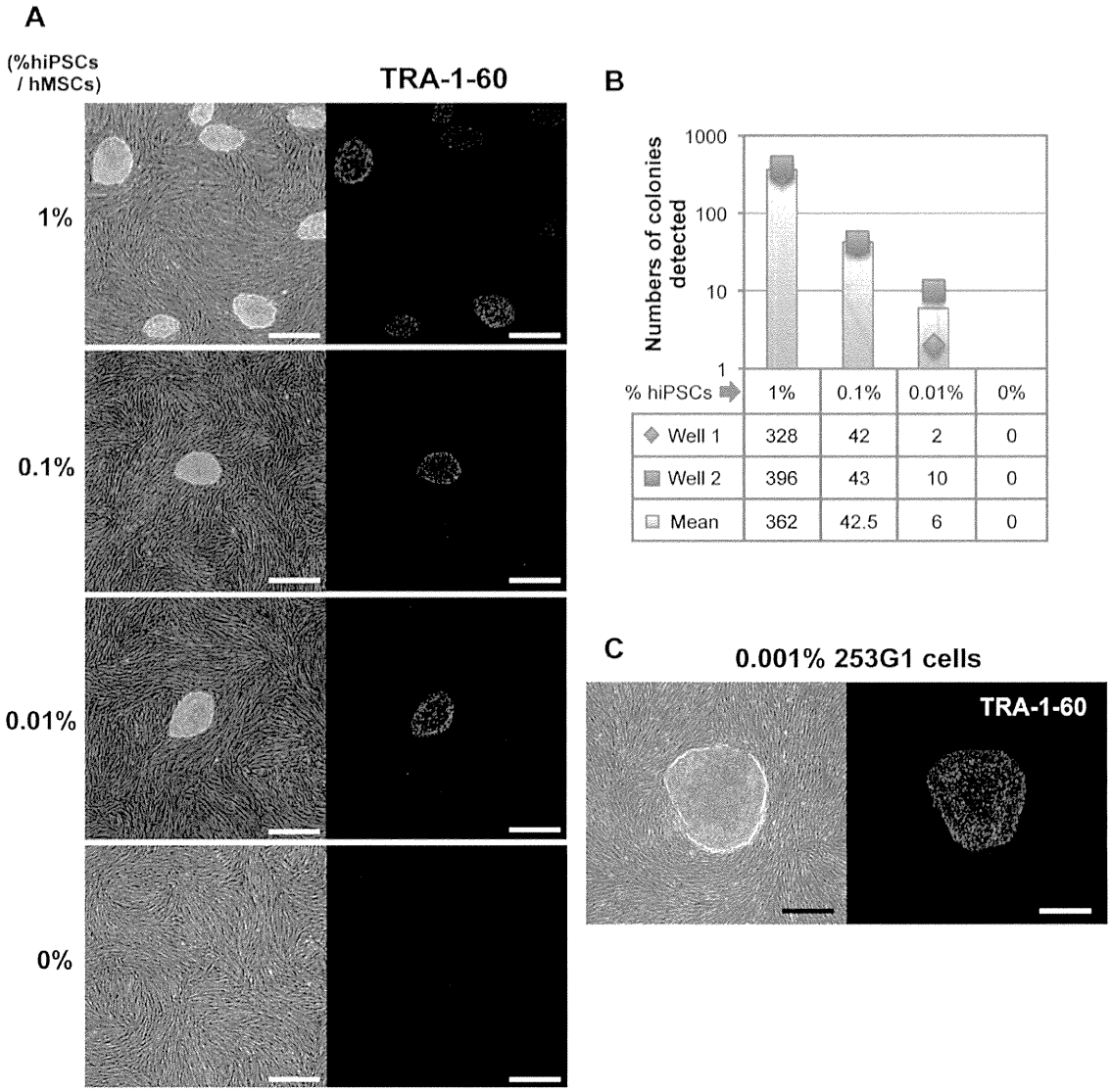

Figure 4. Detection of hiPSCs spiked into hMSCs on the culture system using laminin-521 and Essential 8 medium. (A) Morphologies of forming colonies derived from 409B2 cells spiked into hMSCs are shown (images in the left). 409B2 cells (1%, 1000 cells; 0.1%, 100 cells; 0.01%, 10 cells; 0%, 0 cells) were spiked into hMSCs (100,000 cells) and co-cultured on laminin-521-coated wells in 6-well plates in Essential 8 medium for 7 days. Expression of the undifferentiated marker, TRA-1-60, in these colonies was assessed using immunofluorescence staining (images in the right). Each experiment was carried out in duplicate. Scale bars, 500 μm. (B) Numbers of the colonies detected in each spiked sample in (A) are shown. Data are present as raw data in each well (shown by plots) or the mean of well 1 and well 2 (shown by bar graphs). (C) Morphology of a forming colony derived from 253G1 cells spiked into hMSCs at the ratio of 0.001% (6 hiPSCs to 600,000 hMSCs) is shown (images in the left). Mixture of those cells was co-cultured on a 100-mm cell culture dish coated with laminin-521 in Essential 8 medium for 9 days. Forming colony was stained with anti TRA-1-60 antibody (images in the right). Experiment was carried out in duplicate. Scale bars, 500 μm.
doi:10.1371/journal.pone.0110496.g004

tested another hiPSC line, 253G1, for undifferentiated cells spiked into hMSCs. We found that 253G1 cells spiked into hMSCs at the ratio of 1% and 0.1% formed approximately 100 and 20 colonies, respectively, on laminin-521 in Essential 8 medium (Figure S4). We detected one colony when 253G1 cells were spiked into hMSCs at a ratio of 0.01% or 0.001% and co-cultured on a laminin-521-coated dish in Essential 8 medium (Figure S4 and Figure 4C). Taken together, our culture system using laminin-521 and Essential 8 medium allows the direct detection of 0.001%–0.01% hiPSCs in hMSCs as a result of efficient cell amplification.

We also confirmed that no colonies were detected when a mixture of hiPSCs and hMSCs were cultured on laminin-521 in MSCGM medium instead of Essential 8 medium. In the absence of laminin-521, several colonies were detected in Essential 8 when hMSCs contained 1% hiPSCs but not when hMSCs contained 0.1% and 0.01% hiPSCs (data not shown). These results suggest that laminin-521 is required to detect trace amounts of hiPSCs in hMSCs (less than 0.1%).

To know whether this culture system also works in detecting trace amounts of hiPSCs contaminating other types of cells besides

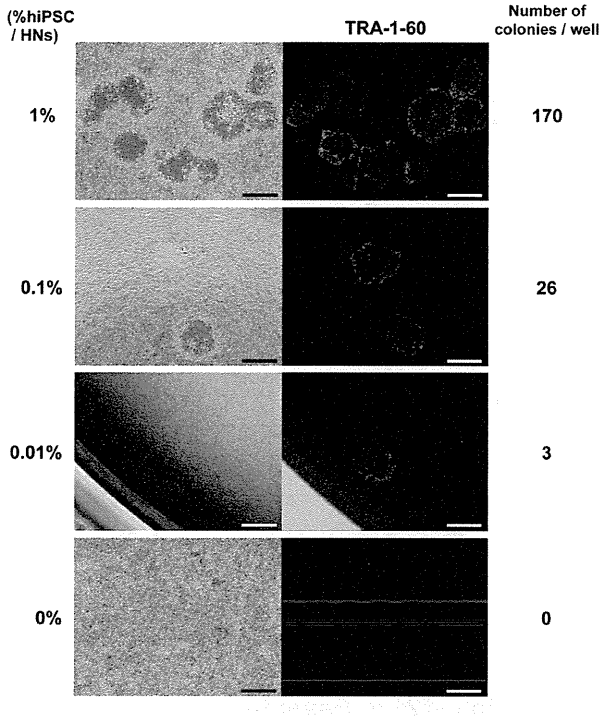

Figure 5. Detection of hiPSCs spiked into human neurons on the culture system using laminin-521 and Essential 8 medium. Morphologies of forming colonies derived from 253G1 cells spiked into human neurons are shown (images in the left). 253G1 cells (1%, 1000 cells; 0.1%, 100 cells; 0.01%, 10 cells; 0%, 0 cells) were spiked into human neurons (100,000 cells) and co-cultured on laminin-521-coated wells in 12-well plates in Essential 8 medium for 6 days. Forming colonies were stained with anti TRA-1-60 antibody (images in the right). HNs, human neurons. Scale bars, 500 μm.
doi:10.1371/journal.pone.0110496.g005

hMSCs, we next tested colony formation of hiPSCs spiked into primary human neurons. Spiked 253G1 cells were co-cultured with human neurons on laminin-521 in Essential 8 medium and clearly formed colonies (Figure 5), which is consistent with the observation using hiPSCs spiked into hMSCs. We detected 170, 26 and 3 colonies that were positive for TRA-1-60 when 253G1 cells were spiked into 1×10^5 human neurons at the ratio of 1, 0.1 and 0.01%, respectively. There was no colony when only human neurons were cultured on our system. These results suggest that this culture system is also useful for detection of trace amounts of hiPSCs not only in hMSCs but also in other types of cells such as human neurons. We also confirmed that no colonies were formed on the well that was not coated with laminin-521 even when human neurons containing 10% hiPSCs were plated (data not shown), indicating that formation of the colonies derived from hiPSCs in human neurons is dependent on laminin-521.

Culture system using laminin-521 and Essential 8 medium has a capacity for direct detection of residual undifferentiated cells contained in differentiating hiPSC cultures

Finally, we examined whether this culture system using laminin-521 and Essential 8 medium is applicable in direct detection of residual hiPSCs contained in differentiated cells derived from hiPSCs. We attempted to differentiate 253G1 cells into MSCs as described in Materials and Methods (Figure 6A). Using this protocol, we observed attached cells with fibroblast-like morphology at the stage of passage 0 MSCs. We confirmed that approximately 20% of these attached cells were positive for staining with anti-CD105 antibody, a MSC marker antibody (Figure S5). During the differentiation process of 253G1 cells into MSCs, we examined the expression levels of residual pluripotency markers in the cell cultures. qRT-PCR analysis revealed that expression of *OCT3/4*, *NANOG* and *LIN28* mRNA were clearly decreased in a time-dependent manner, however, expression levels at the same time point varied markedly among those genes (Figure 6B). In the cells at day 6 of differentiation, mRNA levels of *OCT3/4*, *NANOG* and *LIN28* were 7.3%, 4.8% and 86.4% of the control at day 1, respectively (Figure 6B). At day 14 of differentiation, although *OCT3/4* and *LIN28* were still at detectable levels of 2.6% and 17.2% of control cells, respectively, *NANOG* expression was not detected. These results indicate that the population of residual hiPSCs in differentiating cells, when estimated by the qRT-PCR data, greatly varies and depends on the pluripotency marker gene employed for the estimation. In addition, it is also possible that all the qRT-PCR signals were derived from partially differentiated cells, not from fully undifferentiated cells. To examine colony formation of residual undifferentiated cells in differentiating cell culture, cells at day 6 were dissociated into single cells and replated on laminin-521 in Essential 8 medium. Small cell clusters began to emerge 4 days after plating, rapidly expanded and formed colonies on laminin-521 in Essential 8, while other types of cells gradually decreased their numbers (Figure 6D). After 8 days of culture, 9.5 colonies (the mean of duplicate measurements) were formed from differentiating cells (5×10^4) (Figure 6C) and they were all positive for TRA-1-60 (Figure 6D), indicating that the colonies were derived from residual undifferentiated cells in the differentiating cell cultures. These results suggest that the culture method using a combination of laminin-521 and Essential 8 directly detects residual undifferentiated cells by highly efficient cell amplification. Based on our finding that approximately 0.3 and 6.7 colonies were formed from 1×10^4 MSCs containing 0.01% and 0.1% of 253G1 cells, respectively, in this culture system (Figure S4), and assuming that the sensitivity of the system for hPSCs in EBs are comparable to that in MSCs, the population of the undifferentiated cells in the differentiating cell cultures on day 6 (1.9 colonies/10^4 cells) was estimated to be in between 0.01% and 0.1%. When we tested colony formation using cell cultures on day 14 of differentiation, no colonies were detected on laminin-521 in Essential 8 medium (Figure 6C and data not shown), suggesting that the population of the residual hiPSCs was less than 0.01%.

Discussion

A method to detect residual undifferentiated hPSCs contained in CTPs is required to evaluate product quality during manufacturing processes. In the present study, we propose a novel method to detect a trace amount of undifferentiated hPSCs by highly efficient amplification of those cells *in vitro*. We showed that Essential 8 medium significantly promotes cell growth of hiPSCs dissociated into single cells on laminin-521 compared with the conventional medium, mTeSR1. In addition, Essential 8 medium allowed robust proliferation of hiPSCs even at low cell density on laminin-521. We also demonstrated that 0.001%–0.01% hiPSCs spiked into primary hMSCs were clearly detected and formed colonies on laminin-521 in Essential 8. Similarly, we confirmed that 0.01% hiPSCs spiked into primary human neurons were also detectable on this system. Moreover, we showed that residual undifferentiated hiPSCs contained in differentiating cells were

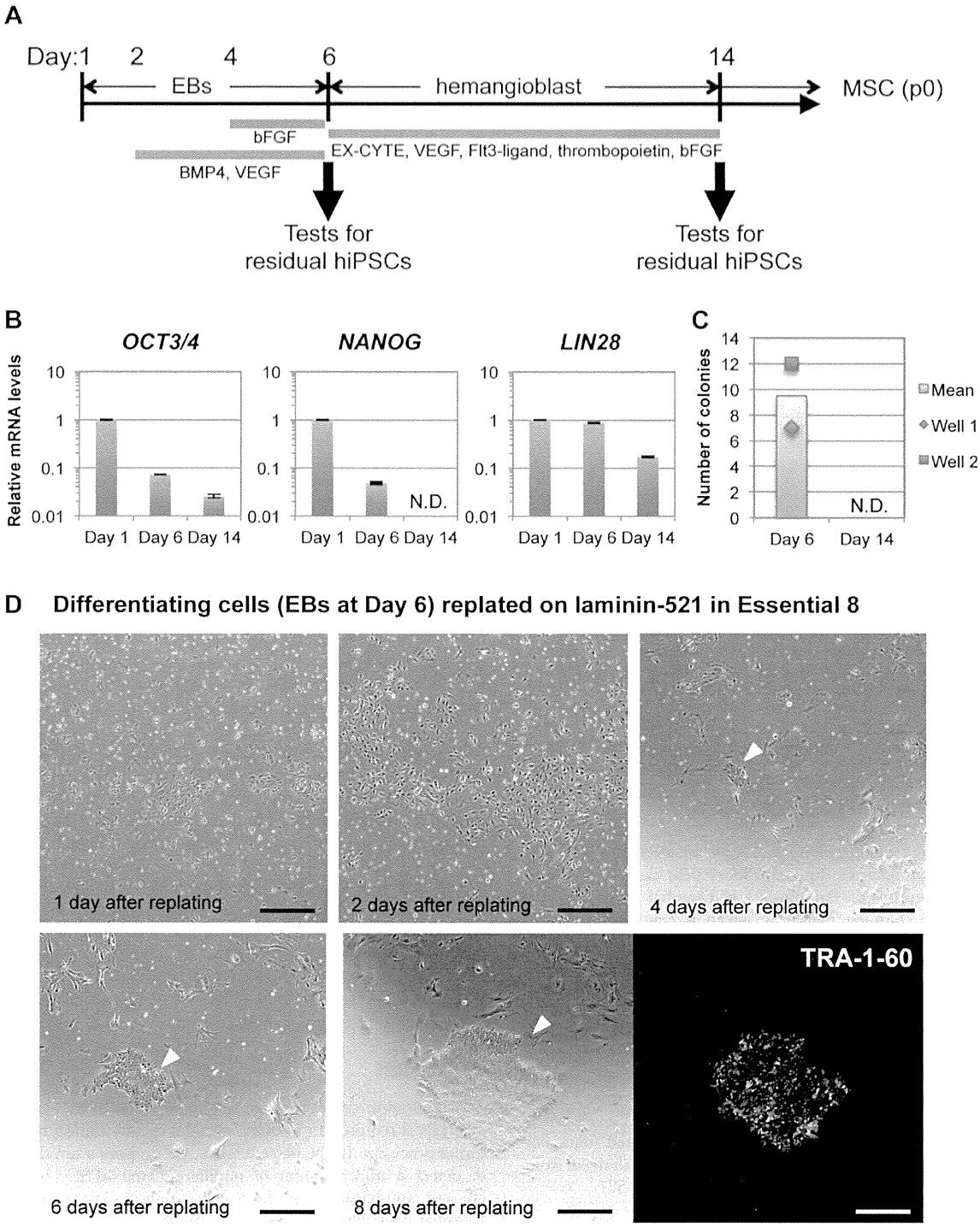

Figure 6. Detection of residual undifferentiated cells contained in differentiating cell cultures. (A) Differentiation scheme of 253G1 cells into MSCs is shown. (B) Expression levels of undifferentiated cell markers (*OCT3/4, NANOG* and *LIN28*) in each cell culture were determined using qRT-PCR. Relative mRNA expression levels are presented as ratios to the level of that in 253G1 cells at Day 1. Results are the mean ± SD (n = 3). (C) Numbers of the forming colonies derived from residual undifferentiated cells in differentiating cell culture at Day 6 or Day 14 are shown. Experiments were carried out in duplicate. Data are present as raw data in each well (shown by plots) or the mean of well 1 and well 2 (shown by bar graphs). (D) Phase contrast images of forming colonies derived from residual undifferentiated cells are shown. Cells at Day 6 of differentiation (EBs) were dissociated into single cells by Accutase and cultured on laminin-521-coated wells in Essential 8 medium (5×10^4/well). After 4 days of culture, small clusters emerged and then started to grow rapidly. Finally, they formed colonies that were positive for TRA-1-60 (shown by immunofluorescence staining, green). Arrowheads indicate a colony derived from same origin. Scale bars, 500 μm.
doi:10.1371/journal.pone.0110496.g006

detectable by forming colonies on laminin-521 in Essential 8 in the process of hMSC differentiation. These results indicate that a culture system utilizing a combination of laminin-521 and Essential 8 medium provides a direct and highly sensitive method for detecting undifferentiated hPSCs. To our knowledge, this is the first report to show a direct and highly-sensitive *in vitro* method for detecting undifferentiated hPSCs as impurities in CTPs.

In this study, highly efficient amplification of undifferentiated hPSCs has been uniquely applied to quality control of CTPs. Amplified hPSC colonies were visible using phase-contrast microscopy and also immunofluorescence staining using pluripotency antibodies, which enabled direct detection of hPSCs contaminating CTPs. Our method distinguished between undifferentiated cells and other cells *in vitro*, and overcame the disadvantage of other *in vitro* methods such as flow cytometry and qRT-PCR. The flow cytometry analysis detects known marker molecules expressed in undifferentiated hPSCs using antibodies and proteins. Signals originating from non-specific detection commonly affect sensitivity of the assay as background. Our *in vitro* method can lower the background arising from non-specific detection and is expected to specifically detect residual undifferentiated hPSCs in CTPs. The qRT-PCR method is highly sensitive and can rapidly quantify undifferentiated cell contamination in CTPs. However, in the present study, gene expression levels of pluripotency markers during the differentiation process of hiPSCs into MSCs varied markedly among those marker genes (Figure 6B). Moreover, there remains a possibility that expression signals of marker genes were not derived from totally undifferentiated hPSCs, but from partially differentiated cells. Indeed, the expression level of *LIN28* did not decrease so much during the differentiation as those of the other genes, which was not obviously associated with the differentiation status of the cells in EBs on Day 6 (Figure 6B), although we have previously reported that *LIN28* was a useful marker for monitoring the level of residual hiPSCs in RPE cells derived from hiPSCs [3]. Thus, it is difficult to determine the presence of residual hiPSCs simply by qRT-PCRs. In contrast, direct detection method using the highly efficient amplification system can clearly detect the presence of intact undifferentiated cells. Based on the result from direct detection of residual hiPSCs when tested the cells on Day 6 of differentiation (approximately 0.01%–0.1%) (Figure 6C-D), it is conceivable that the qRT-PCR signals for the pluripotency marker genes (Figure 6B) are partly derived from residual hiPSCs but mainly derived from partially differentiated cells. Similarly, in the case of the cells at Day 14 of differentiation, the majority of the qRT-PCR signals of *OCT3/4* and *LIN28* (Figure 6B) are considered to be attributable to partially differentiating cells but not to intact hiPSCs. Combination of the *in vitro* methods including our cell culture method would mutually support useful quality assessment of CTPs to detect undifferentiated hPSCs.

In addition to the detection of undifferentiated cells, this culture system using laminin-521 and Essential 8 medium allows further characterization of the undifferentiated cells if they are maintained *in vitro* or inoculated into immunodeficient animals. Analyses for the properties of the residual undifferentiated cells would be necessary not only for the quality assessment of CTPs, but also for improvement of quality specifications of hPSCs as a raw/intermediate material for production of CTPs.

Here, we showed that our culture system is able to detect 0.01% of 409B2 hiPSCs and 0.001% of 253G1 hiPSCs, both of which were spiked into hMSCs (Figure 4). The detection sensitivity for hiPSCs spiked into hMSCs was different between the two hiPSC lines, although such a difference in cell growth on laminin-521 was not found between these two cell lines (Figure 3). This difference may be attributable to the difference in the growth potential of hPSCs in the specific environment provided by CTPs. Kanemura *et al.* have recently demonstrated that hiPSCs co-cultured with iPSC-derived RPE undergo apoptosis by pigment epithelium-derived factor (PEDF) secreted from hiPSC-derived RPE [15], showing that CTPs themselves have the potential to affect cell growth of hPSCs. In the present study, the influence of the co-culture system with hMSCs to the proliferation of hiPSCs might have been different between the two cell lines.

The mechanism by which laminin-521 and Essential 8 medium enhance hiPSCs cell proliferation remains unclear. Rodin *et al.* have recently shown that addition of E-cadherin to laminin-521 permitted the efficient clonal expansion of hESCs [7]. E-cadherin is known to be the primary cell-cell adhesion molecule and essential for hESC survival [16]. We observed that anti-E-cadherin antibody decreased growth potential of hiPSCs under our experimental conditions (data not shown). Therefore, E-cadherin signaling may play some important roles in the rapid cell growth on laminin-521 in Essential 8 medium.

Tumorigenicity is one of the major safety concerns for CTPs derived from hPSCs that are transplanted into patients. However, testing strategies for the tumorigenicity of hPSC-derived CTPs have not yet been established. Here, we introduced a novel testing method for directly detecting a trace amount of undifferentiated hPSCs *in vitro*. The ability of each tumorigenicity-associated test should be taken into consideration to evaluate tumorigenicity of residual undifferentiated hPSCs as impurities in products. *In vivo* tumorigenicity tests using immunodeficient animals can detect tumorigenic cells including undifferentiated hPSCs, but this method is costly and time-consuming. The flow cytometry analysis and qRT-PCR are rapid, but these methods indirectly detect tumorigenic cells depending on marker molecules. Risk of tumorigenicity in hPSCs-derived CTPs should be assessed, based on the results from an appropriate combination of these tumorigenicity-associated tests. Our novel method will contribute to establishment of the testing strategies for tumorigenicity in products, following evaluation of the quality of CTPs derived from hPSCs for the future regenerative medicine/cell therapy.

Supporting Information

Figure S1 (A) Quantification of the number of dissociated 201B7 cells expanded on laminin-521 or Matrigel in Essential 8 or mTeSR1 medium. Data are presented as the mean ± standard deviation (SD) of three independent experiments (**$P<0.01$, two-way ANOVA followed by a Bonferroni post-hoc test). LN521, laminin-521. MG, Matrigel. (B) Quantification of the number of dissociated 201B7 cells expanded on laminin-521 or LM511-E8 in Essential 8 or mTeSR1 medium. Results are presented as the mean ±SD (n = 3) (***$P<0.001$, two-way ANOVA followed by a Bonferroni post-hoc test).
(TIF)

Figure S2 (A-B) Expression levels of undifferentiated markers (*OCT3/4, NANOG, SOX2* and *LIN28*) in 201B7 cells (A) and 409B2 cells (B) subcultured on laminin-521 in Essential 8 were determined using qRT-PCR. Relative mRNA expression levels are presented as ratios to the level of that in control cells subcultured on Matrigel in mTeSR1 medium by colony passage. Results are presented as the mean ± SD (n = 3). (C-D) Expression levels of markers for the differentiation of embryoid bodies (EBs) derived from 201B7 cells (C) and 409B2 cells (D): endoderm (*GATA6, SOX17*), mesoderm (*CDH5, FOXF1*), and ectoderm (*SOX1, PAX6*). Relative mRNA expression levels are presented as

ratios to the level of that in control cells (EBs at day 10). Results are presented as the mean ± SD (n = 3).
(TIF)

Figure S3 Quantification of the number of 253G1 cells expanded on laminin-521 in Essential 8 or mTeSR1 medium. Cell numbers were counted at day 6, 9, and 12 after plating at 8.0×10^3 cells/cm^2 or 8.0×10^2 cells/cm^2.
(TIF)

Figure S4 Morphologies of forming colonies derived from 253G1 cells spiked into hMSCs are shown (images in the left). 253G1 cells (1%, 300 cells; 0.1%, 30 cells; 0.01%, 3 cells; 0%, 0 cells) were spiked into hMSCs (30,000 cells) and co-cultured on 12-well plates coated with laminin-521 in Essential 8 medium for 9 days. Expression of the undifferentiated cell marker, TRA-1-60, in these colonies was assessed using immunofluorescence staining (images to the right). Each experiment was carried out in duplicate.
(TIF)

Figure S5 Phase contrast images of the cells at day 18 of differentiation (at the stage of passage 0 MSCs) are shown. Expression of MSC marker, CD105, in these cells was examined using immunofluorescence staining (images to the right). Arrowheads indicate the cells that were positive for CD105.
(TIF)

Table S1 Sequences of the primers and probes for qRT-PCR.
(DOCX)

Acknowledgments

This work was supported by Research Grants from the Japanese Ministry of Health, Labour and Welfare (H23-SAISEI-IPPAN-004, H23-SAISEI-IPPAN-005, H24-IYAKU-SHITEI-027, H25-JITSUYOKA(SAISEI)-IPPAN-008, and Marketing Authorization Facilitation Program for Innovative Therapeutic Products).

Author Contributions

Conceived and designed the experiments: KT SY YS. Performed the experiments: KT. Analyzed the data: KT SY TK HS AU YS. Contributed reagents/materials/analysis tools: KT SY TK HS AU YS. Wrote the paper: KT SY YS. Acquired the funding: HS AU YS.

References

1. Bailey AM (2012) Balancing tissue and tumor formation in regenerative medicine. Sci Transl Med 4: 147fs28. Rev.
2. Kuroda T, Yasuda S, Sato Y (2013) Tumorigenicity studies for human pluripotent stem cell-derived products. Biol. Pharm. Bull 36: 189–192.
3. Kuroda T, Yasuda S, Kusakawa S, Hirata N, Kanda Y, et al. (2012) Highly sensitive in vitro methods for detection of residual undifferentiated cells in retinal pigment epithelial cells derived from human iPS cells. PLoS One 7: e37342.
4. Food and Drug Administration (2008) Cellular Therapies derived from Human Embryonic Stem Cells-Considerations for Pre-Clinical Safety Testing and Patient Monitoring-April 2008. Cellular, Tissue, and Gene Therapies Advisory Committee (CTGTAC) Meeting #45. Available: <http://www.fda.gov/ohrms/dockets/ac/08/briefing/2008-0471B1_1.pdf>.
5. Hentze H, Soong PL, Wang ST, Phillips BW, Putti TC, et al. (2009) Teratoma formation by human embryonic stem cells: evaluation of essential parameters for future safety studies. Stem Cell Res 2: 198–210.
6. Watanabe K, Ueno M, Kamiya D, Nishiyama A, Matsumura M, et al. (2007) A ROCK inhibitor permits survival of dissociated human embryonic stem cells. Nat. Biotechnol 25: 681–686.
7. Rodin S, Antonsson L, Niaudet C, Simonson OE, Salmela E, et al. (2014) Clonal culturing of human embryonic stem cells on laminin-521/E-cadherin matrix in defined and xeno-free environment. Nat. Commun 5: 3195.
8. Miyazaki T, Futaki S, Suemori H, Taniguchi Y, Yamada M, et al. (2012) Laminin E8 fragments support efficient adhesion and expansion of dissociated human pluripotent stem cells. Nat. Commun 3: 1236.
9. Chen G, Gulbranson DR, Hou Z, Bolin JM, Ruotti V, et al. (2011) Chemically defined conditions for human iPSC derivation and culture. Nat. Methods 8: 424–429.
10. Chambers SM, Fasano CA, Papapetrou EP, Tomishima M, Sadelain M, et al. (2009) Highly efficient neural conversion of human ES and iPS cells by dual inhibition of SMAD signaling. Nat. Biotechnol 27: 275–280.
11. Kajiwara M, Aoi T, Okita K, Takahashi R, Inoue H, et al. (2012) Donor-dependent variations in hepatic differentiation from human-induced pluripotent stem cells. Proc Natl Acad Sci U S A 109: 12538–12543.
12. Jung Y, Bauer G, Nolta JA (2012) Concise review: Induced pluripotent stem cell-derived mesenchymal stem cells: progress toward safe clinical products. Stem Cells 30: 42–47.
13. Chen YS, Pelekanos RA, Ellis RL, Horne R, Wolvetang EJ, et al. (2012) Small molecule mesengenic induction of human induced pluripotent stem cells to generate mesenchymal stem/stromal cells. Stem Cells Transl Med 1: 83–95.
14. Kimbrel EA, Kouris NA, Yavanian G, Chu J, Qin Y, et al. (2014) Mesenchymal stem cell population derived from human pluripotent stem cells displays potent immunomodulatory and therapeutic properties. Stem Cells Dev 23: 1611–1624.
15. Kanemura H, Go MJ, Nishishita N, Sakai N, Kamao H, et al. (2013) Pigment epithelium-derived factor secreted from retinal pigment epithelium facilitates apoptotic cell death of iPSC. Sci Rep 3: 2334.
16. Xu Y, Zhu X, Hahm HS, Wei W, Hao E, et al. (2010) Revealing a core signaling regulatory mechanism for pluripotent stem cell survival and self-renewal by small molecules. Proc Natl Acad Sci U S A 107: 8129–8134.
17. Takahashi K, Tanabe K, Ohnuki M, Narita M, Ichisaka T, et al. (2007) Induction of pluripotent stem cells from adult human fibroblasts by defined factors. Cell 131: 861–872.
18. Nakagawa M, Koyanagi M, Tanabe K, Takahashi K, Ichisaka T, et al. (2008) Generation of induced pluripotent stem cells without Myc from mouse and human fibroblasts. Nat. Biotechnol 26: 101–106.
19. Okita K, Matsumura Y, Sato Y, Okada A, Morizane A, et al. (2011) A more efficient method to generate integration-free human iPS cells. Nat. Methods 8: 409–412.